Downloaded from gsabulletin.gsapubs.org on July 6, 2010

Oligocene–Miocene basin evolution in the northern Altiplano, Bolivia: Implications for evolution of the central Andean backthrust belt and high plateau

Bryan P. Murray[1,†], Brian K. Horton[2] , Ramiro Matos[3], and Matthew T. Heizler[4]
[1]*Department of Earth Science, University of California, Santa Barbara, Webb Hall, Santa Barbara, California 93106-9630, USA*
[2]*Institute for Geophysics and Department of Geological Sciences, Jackson School of Geosciences, University of Texas at Austin, Austin, Texas 78712, USA*
[3]*Instituto de Investigaciones Geológicas y Medio Ambiente, Universidad Mayor de San Andrés, Casilla Postal 4787, La Paz, Bolivia*
[4]*New Mexico Bureau of Geology and Mineral Resources, Socorro, New Mexico 87801, USA*

ABSTRACT

The upper Oligocene to lower Miocene Peñas and Aranjuez formations are exposed in north-northwest–trending outcrop belts of the central Andean backthrust belt situated within the central Andean plateau along the boundary between the northern Altiplano and the Eastern Cordillera of Bolivia. Sedimentary lithofacies analyses indicate that these coarse-grained siliciclastic formations were deposited primarily in alluvial fan to braided fluvial environments. An upsection change from principally fine-grained sandstone to cobble conglomerate is consistent with increased proximity to the sediment source with time. Paleocurrent analyses reveal that flow was predominantly directed toward the west-southwest away from Cordillera Real, the elevated core of the Eastern Cordillera. Provenance data from conglomerate clast compositions and sandstone petrofacies suggest derivation from recycled quartz-rich metasedimentary and sedimentary rocks from the Paleozoic section in the Eastern Cordillera. The paleoflow orientations, sediment provenance, and increased proximity of the sediment source suggest that deposition of the Peñas and Aranjuez formations was related to surface uplift of the Eastern Cordillera relative to the Altiplano. Growth strata observed in the Aranjuez Formation further indicate that shortening was synchronous with deposition, probably in a hinterland basin. New $^{40}Ar/^{39}Ar$ ages from a lowermost exposed igneous unit and interbedded ash-fall tuff beds in the Aranjuez and Peñas formations show that synorogenic sedimentation and fold-thrust deformation in the frontal (west-southwestern) zone of the central Andean backthrust belt was concentrated during late Oligocene–early Miocene time. These age results are consistent with previous studies of east-derived sedimentation in the Altiplano and indicate regional uplift of the Eastern Cordillera at this time. Upsection trends in provenance data further suggest a progressively greater contribution from younger Paleozoic strata, possibly due to activation of new thrust faults during west-southwestward propagation of the backthrust belt toward the Altiplano. Such a progression of late Oligocene–early Miocene shortening along the Altiplano–Eastern Cordillera boundary likely reflects significant crustal thickening, potential isostatic uplift, and initial topographic expression of the eastern margin of the central Andean plateau.

INTRODUCTION

Located in the central portion of the ~8000-km-long Andean orogenic belt, the Altiplano is one of the largest continental plateaus on Earth. The Andes are the topographic expression of Cenozoic contractional stain associated with subduction along the western margin of South America (Fig. 1; Isacks, 1988), yet the mechanisms for uplifting the central Andes and Altiplano are not well understood. The high elevation of the central Andean plateau is isostatically supported by up to 70-km-thick crust (e.g., Beck et al., 1996). Some have suggested that continuous eastward propagation of a fold-thrust belt, including a west-directed backthrust belt and east-directed basement-involved megathrust sheets, was the cause of crustal thickening, deformation, and observed topographic patterns in the central Andes (e.g., Horton et al., 2001; McQuarrie, 2002; DeCelles and Horton, 2003; McQuarrie et al., 2005; McQuarrie et al., 2008). Other studies have proposed that plateau uplift resulted from deeper processes such as thickening of thermally weakened lower crust by ductile horizontal shortening and magmatic addition (e.g., Isacks, 1988; Allmendinger et al., 1997) or from rapid removal of a dense lower lithospheric root (e.g., Garzione et al., 2006; Ghosh et al., 2006; Garzione et al., 2008; Hoke and Garzione, 2008).

The timing of crustal shortening in the central Andes remains relatively poorly constrained. Previous workers have suggested initial deformation and possible early plateau uplift between 30 and 25 Ma on the basis of a late Oligocene to early Miocene influx of synorogenic sediment to the Altiplano and Andean foreland basin (Isacks, 1988; Sempere et al., 1990; Gubbels et al., 1993; Allmendinger et al., 1997). In contrast, paleoelevation studies utilizing stable oxygen isotope data from Neogene basin fill have suggested rapid plateau uplift in late Miocene time (Garzione et al., 2006; Ghosh et al., 2006; Garzione et al., 2008; Hoke and Garzione, 2008). Other studies focusing on thermochronological data (Benjamin et al., 1987; McBride et al., 1987; Farrar et al., 1988; Masek et al., 1994; Barnes et al., 2006; Gillis et al., 2006; Ege et al., 2007; Barnes et al., 2008; McQuarrie et al., 2008) and relict foreland basin deposits (Kennan et al., 1995; Lamb and Hoke, 1997; Horton et al., 2001; DeCelles and Horton, 2003) have proposed initial Andean deformation as early as Late Cretaceous to middle Eocene time.

Despite their differences, these varied interpretations for the mechanisms and timing of shortening and plateau uplift share a

†E-mail: bmurray@umail.ucsb.edu

GSA Bulletin; September/October 2010; v. 122; no. 9/10; p. 1443–1462; doi: 10.1130/B30129.1; 14 figures; 4 tables; Data Repository item 2010105.

For permission to copy, contact editing@geosociety.org
© 2010 Geological Society of America

Downloaded from gsabulletin.gsapubs.org on July 6, 2010

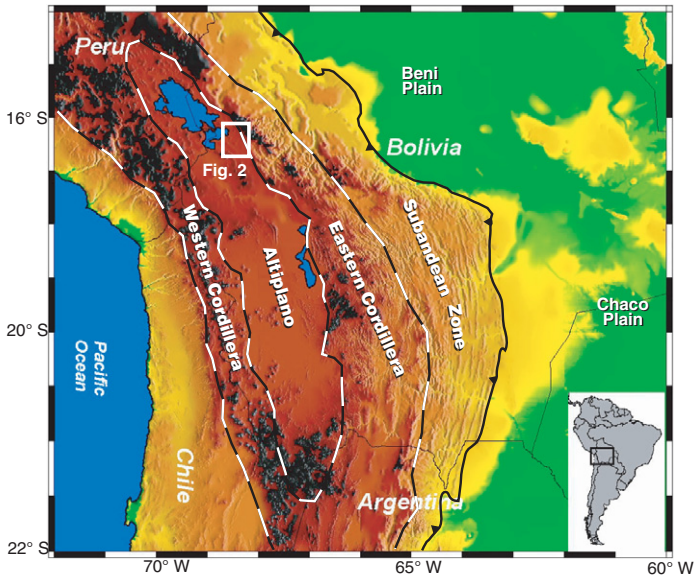

Figure 1. Map showing regional topography of the central Andes. Major physiographic divisions are separated by dashed lines (after Isacks, 1988; McQuarrie et al., 2005). Darker colors (orange, red, gray, black) define regions of higher topography (>3.5 km). Box shows location of Figure 2.

common basis in the consideration of sediment accumulation patterns within and adjacent to the central Andean plateau. For this reason, the spatial and temporal trends in the configuration of individual sedimentary basins, including the age, provenance, burial history, and relationships to upper-crustal structures, are important to any models of deformation and uplift in the central Andes.

The present study of the middle Cenozoic Peñas and Aranjuez formations, siliciclastic deposits exposed in the northeastern Altiplano of Bolivia, helps constrain the history of initial hinterland basin development in the central Andean plateau and relative surface uplift along the plateau margin. Although previous studies have focused on synorogenic sedimentary deposits exposed in the Altiplano and Eastern Cordillera (e.g., Sempere et al., 1990; Kennan et al., 1995; Lamb and Hoke, 1997; Horton, 1998; Horton et al., 2002; DeCelles and Horton, 2003; Horton, 2005), there has been limited research on the basin-fill exposures in closest proximity to the Cordillera Real, the range with the highest peaks and greatest concentration of thermochronological data in the Eastern Cordillera (Benjamin et al., 1987; McBride et al., 1987; Farrar et al., 1988; Gillis et al., 2006). This study presents new results from an investigation of the sedimentology, provenance, and $^{40}Ar/^{39}Ar$ chronology of the Peñas and Aranjuez formations along the northeastern edge of the Altiplano adjacent to the Eastern Cordillera in order to determine the relationship of these deposits to upper-crustal deformation and topographic development along the margins of the central Andean plateau.

GEOLOGIC SETTING

The central Andes in Bolivia can be subdivided into five physiographically distinct provinces (from west to east): the Western Cordillera, the Altiplano, the Eastern Cordillera, the Subandean Zone, and the Beni-Chaco Plain (Fig. 1; Isacks, 1988). The Altiplano is an internally drained, ~200-km-wide region of low topographic relief located in the hinterland of the central Andean fold-thrust belt with an average elevation of 3.8 km. Bounding the Altiplano are the Eastern Cordillera, which represents the uplifted core of the Andean fold-thrust belt, and the Western Cordillera, the location of the active magmatic arc. Both of these systems rise to peak elevations >6 km. Located farther east is the Subandean Zone, the frontal region of the active fold-thrust belt, and the Beni-Chaco Plain, the modern retroarc foreland basin (Isacks, 1988; Jordan, 1995; Horton and DeCelles, 1997; Lamb and Hoke, 1997).

The Altiplano basin contains a thick succession (up to 12 km) of regionally extensive Upper Cretaceous through Cenozoic sedimentary and volcanic rocks derived from either the Western Cordillera or Eastern Cordillera. The stratigraphy of the Altiplano can be summarized as follows: (1) a 250–900-m-thick lower succession of Maastrichtian to mid-Paleocene carbonate (El Molino Formation) and east-derived, distal-fluvial siltstone and sandstone (Santa Lucia Formation); (2) a 3000–6500-m-thick middle succession of upper Eocene to Oligocene west-derived fluvial sandstone (Potoco Formation); (3) a 1000–4000-m-thick upper succession of poorly dated, partially Potoco-age–equivalent (Oligocene to middle Miocene), east-derived fluvial and alluvial fan conglomerate (Coniri Formation) and numerous upper Oligocene to Quaternary volcaniclastic units (Swanson et al., 1987; Sempere et al., 1990; Kennan et al., 1995; Lamb and Hoke, 1997; Horton et al., 2001; Horton et al., 2002; DeCelles and Horton, 2003). Previous studies have related the observed stratigraphy to an eastward migration of the Andean foreland basin system, with the El Molino and Santa Lucia formations deposited in a backbulge depozone, the main body of the Potoco Formation recording foredeep deposition, and the upper Potoco, Coniri, and younger volcaniclastic formations representing intermontane (hinterland) basin deposition in the Altiplano (DeCelles and Giles, 1996; Horton et al., 2001; Horton et al., 2002; DeCelles and Horton, 2003).

In the northeastern Altiplano, the Peñas and Aranjuez formations form discontinuous outcrops of coarse-grained siliciclastic deposits that trend north-northwest, roughly parallel to tectonic strike in the adjacent Eastern Cordillera (Fig. 2). The basal contacts of these formations are in angular unconformity above Devonian strata. The Peñas Formation is up to ~1100 m thick and is best exposed near the town of Peñas (Fig. 3A) and at Cerro Santa Ana, north of the La Paz and El Alto metropolitan areas (Fig. 3B). Numerous smaller outcrops of the Peñas Formation with limited exposure are also present in the region northwest of La Paz (Fig. 2). The Aranjuez Formation is >340 m thick and is exposed south of La Paz near Zona Sur, Pedregal (Fig. 3C), Jankho Khaua, and east of Rio La Paz (Fig. 2). The Peñas and Aranjuez formations have been previously mapped as separate units based solely on outcrop location; however, based on their proximity, similar lithofacies, and presumed age, they are considered to be stratigraphic equivalents (e.g., Lohmann, 1970; GEOBOL, 1995b) and also have been associated with the Luribay and Salla formations located >100 km to the south-southeast (e.g., Gillis et al., 2004, 2006).

Potential sediment sources for the northern Altiplano basin include principally Paleozoic sedimentary rocks exposed in the central

Downloaded from gsabulletin.gsapubs.org on July 6, 2010

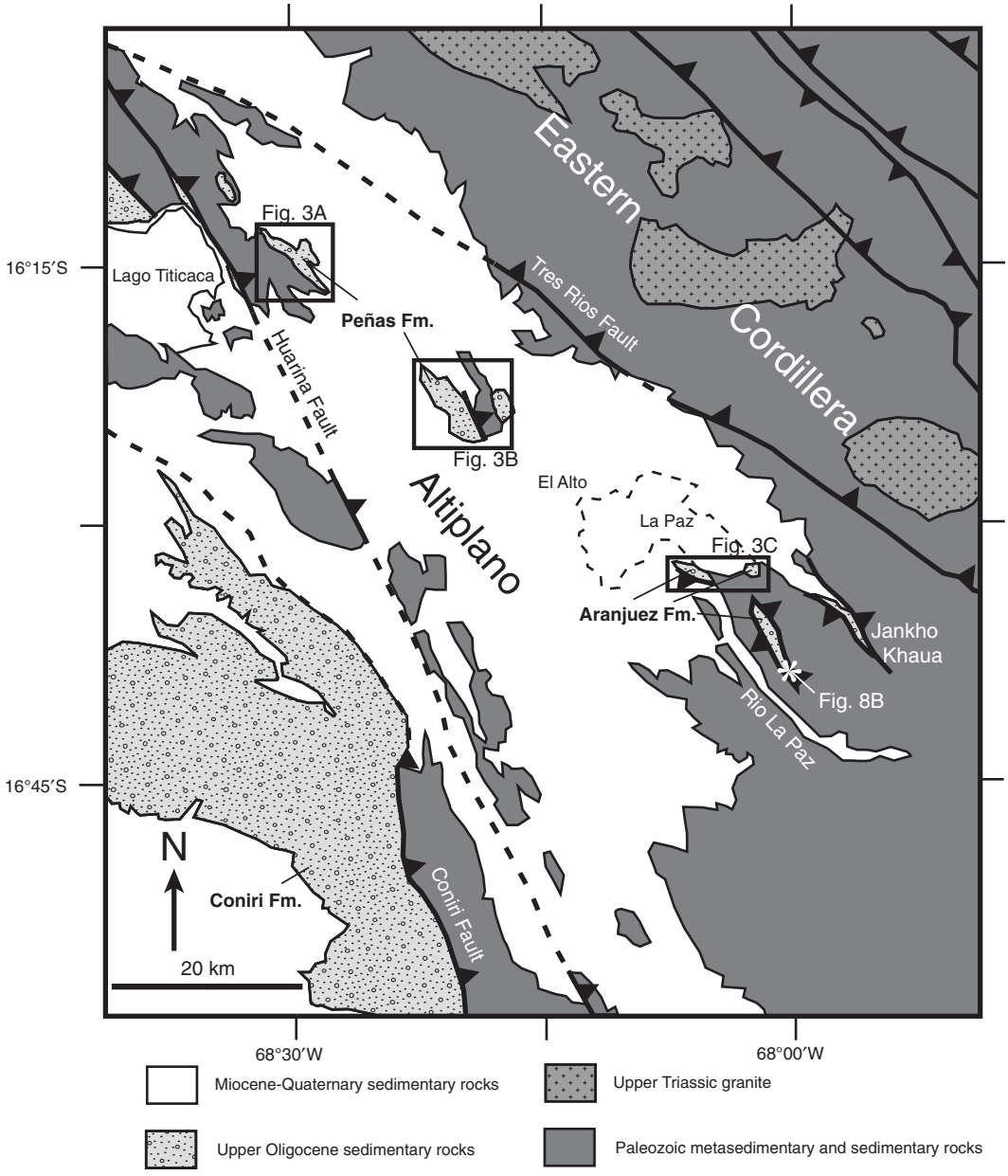

Figure 2. Regional geologic map of the La Paz (Bolivia) region along the Eastern Cordillera–Altiplano boundary showing the generalized geologic units and major faults (simplified from SERGEOMIN, 1997). Boxes show locations of Figure 3. Asterisk denotes location of photograph in Figure 8B.

Andean backthrust belt of the easternmost Altiplano and Eastern Cordillera and principally Cenozoic igneous rocks of the Western Cordillera. The Eastern Cordillera is a 200-km-wide range that creates a drainage divide between the Altiplano and the river networks that flow eastward toward the South American craton. The Eastern Cordillera at 16° S–18° S is composed primarily of Ordovician–Carboniferous sedimentary and low-grade metasedimentary rocks with local exposures of Cretaceous–Cenozoic strata, Permo-Triassic and Neogene granitoids, and Jurassic–Cretaceous hypabyssal and volcanic flows (Gubbels et al., 1993; SERGEOMIN, 1997; Horton et al., 2002; DeCelles and Horton, 2003). A continuous succession of Paleozoic marine deposits includes: (1) the Ordovician Coroico (~2300-m-thick) and Amutara (~800- to 3300-m-thick) formations, low-grade metasedimentary units composed of dark-gray to white quartzite, slate, and phyllite; (2) the Ordovician–Silurian Cancañiri Formation (0–150 m thick), a poorly sorted, dark-gray to green diamictite with granite clasts and sandy mudstone; (3) the Silurian Uncia Formation (850–1200 m thick), a unit of black to dark-brown shale and minor siltstone; (4) the Silurian Catavi Formation (500–800 m thick), a thinly interbedded, gray to green sandstone and siltstone unit; (5) the Devonian Vila Vila Formation (700–1700 m thick), a thickly bedded red to purple sandstone with minor shale; (6) the Devonian Belén Formation (1000–1400 m thick), a unit of grayish-green to brown shale and minor sandstone; (7) the Devonian Sica Sica (400- to 600-m-thick) and Colpacucho (500- to 900-m-thick) formations, white to light-brown sandstone with interbedded siltstone; and (8) the Carboniferous Copacabana Formation (15–300 m thick), a unit of limestone, sandstone, and siltstone that occurs locally (GEOBOL, 1995c; Sempere, 1995; González et al., 1996; Suárez and Diaz, 1996; SERGEOMIN, 1997; McQuarrie and DeCelles, 2001).

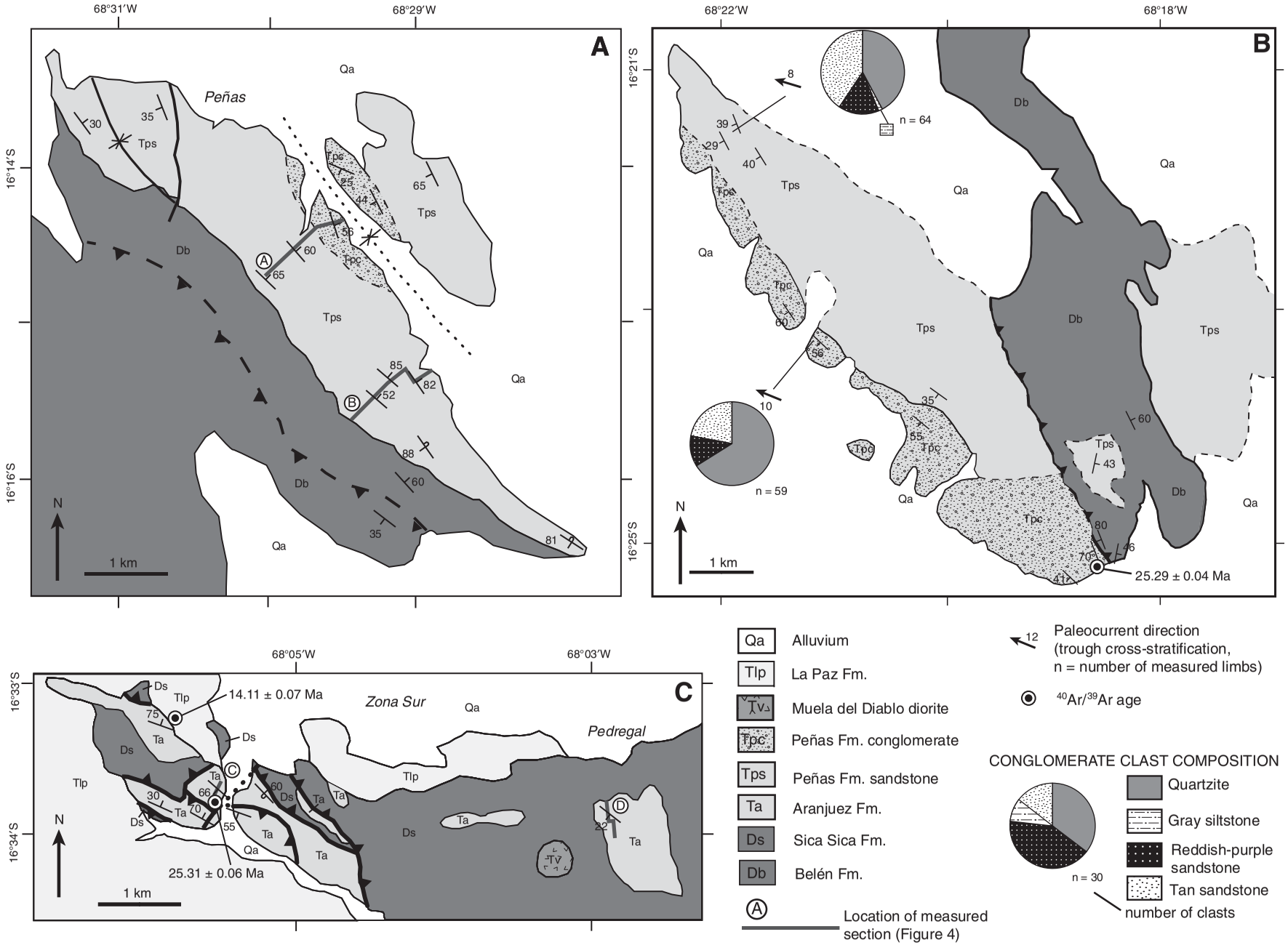

Figure 3. Geologic maps of study sites. (A) Peñas region, showing structural relationships and location of measured sections in the Peñas Formation (modified from GEOBOL, 1995a, 1995c). (B) Cerro Santa Ana region, showing structural relationships, conglomerate clast-count results, and paleocurrent directions for the Peñas Formation (modified from GEOBOL, 1995b). (C) South La Paz region, showing structural relationships and location of measured sections in the Aranjuez Formation (modified from GEOBOL, 1995b).

Downloaded from gsabulletin.gsapubs.org on July 6, 2010
Murray et al.

Downloaded from gsabulletin.gsapubs.org on July 6, 2010

Regionally, the Eastern Cordillera is a bivergent fold-thrust belt with major décollement horizons in the Coroico, Cancañiri, Uncia, and Belén formations (McQuarrie and DeCelles, 2001; McQuarrie, 2002). The eastern portion of the Eastern Cordillera consists primarily of east-northeast–directed thrust faults that expose Silurian–Devonian strata (McQuarrie, 2002; McQuarrie et al., 2008). The westernmost Eastern Cordillera is a region of west-southwest–directed thrust faults, referred to as the central Andean backthrust belt or Huarina fold-thrust belt (e.g., Roeder, 1988; Sempere et al., 1990; McQuarrie and DeCelles, 2001). The central Andean backthrust belt extends from ~15° S to 22° S and consists of Ordovician–Devonian strata with limited exposures of Carboniferous and Cretaceous rocks. Locally, frontal thrusts of the central Andean backthrust belt, including the Huarina and Coniri faults (Fig. 2), place Paleozoic strata over mid-Cenozoic Altiplano basin fill, and deform and uplift Cenozoic strata such as the Peñas and Aranjuez formations unconformably deposited on the hanging wall of these faults (Sempere et al., 1990; SERGEOMIN, 1997). Based on the presence of upper Oligocene to lower Miocene growth strata that are overlapped by slightly deformed younger strata, most upper-crustal shortening in the Eastern Cordillera apparently ceased by ~20–10 Ma when deformation was transferred eastward into the Subandean Zone (Roeder, 1988; Sempere et al., 1990; Gubbels et al., 1993; Lamb and Hoke, 1997; McQuarrie and DeCelles, 2001; Horton, 2005).

Located on the opposing side of the Altiplano, the Western Cordillera is a ~70-km-wide range consisting of Miocene–Quaternary volcanoes and arc-derived ignimbrite sheets (Pareja et al., 1978; Isacks, 1988; Reutter et al., 1994; Wörner et al., 2000a; Horton et al., 2002). Underlying the volcanic cover rocks, the Western Cordillera is composed primarily of Precambrian granitic and gneissic basement. Evidence for this relationship includes outcrops of dated Precambrian rocks beneath volcanic cover (e.g., Troëng et al., 1994; Wörner et al., 2000b), granitic and gneissic xenoliths in Neogene igneous rocks (e.g., Jiménez De Ríos, 1992), Precambrian basement rocks from drill-hole samples (e.g., Lehmann, 1978), and Precambrian granite and gneiss clasts in west-derived middle to upper Tertiary strata in the Altiplano (e.g., Jiménez De Ríos, 1992; Horton et al., 2002).

Although the composition of the Western Cordillera can be inferred from available data, the structural and tectonic history is relatively unknown as a result of the Neogene volcanic cover. Synorogenic sedimentation represented by foreland basin deposits derived from the Western Cordillera suggests that this region may have been the frontal zone of the Andean fold-thrust belt during Eocene time, prior to deformation in the Eastern Cordillera and Subandean Zone (Horton et al., 2002; DeCelles and Horton, 2003).

SEDIMENTOLOGY

Four stratigraphic sections measured in the Peñas and Aranjuez formations provide the basis for the following descriptions of sedimentary lithofacies of individual bedsets and interpretations of depositional processes (Fig. 4 and Table 1). The ten sedimentary lithofacies are grouped into a distinctive collection of four sedimentary lithofacies associations that are interpreted to reflect processes in different depositional environments (Table 2). In the following interpretations, the terms distal, intermediate, or proximal refer to the relative proximity of the basin to the sediment source region.

Peñas Formation

Two stratigraphic sections were measured in the ~1100-m-thick Peñas Formation (Figs. 3A, 4A, and 4B). The base of the Peñas Formation sits in angular unconformity above the underlying Devonian Belén Formation. The Peñas Formation constitutes a progradational coarsening upward package that can be subdivided into three different facies associations attributable to depositional processes in the proximal, medial, and distal portions of a streamflow-dominated alluvial fan system (Table 2) that may have passed downslope into a braided fluvial system.

Lithofacies Association 1: Cross-Stratified Sandstone and Interbedded Mudstone

This lithofacies association (Table 2) comprises the lower ~425 m of the Peñas Formation and is composed of fine- to medium-grained sandstones interbedded with mudstones. Individual sandstone beds are thickly to very thickly bedded (~0.3–1.5 m), extend laterally for tens of meters, and have basal contacts that generally form concave-up irregular erosional surfaces in which the sandstone units cut into underlying mudstone or sandstone beds (Fig. 5A). Interbedded mudstone layers typically occur as lenses a few tens of centimeters in thickness, although locally thicker mudstone layers (up to 18 m) may extend laterally for tens of meters.

Based on the observed lithofacies, this facies association is interpreted as the product of deposition in the distal zone of a streamflow-dominated alluvial fan or a moderate-energy, sandy braided fluvial system (e.g., Miall, 1985, 1996). Upward fining and coarsening trends in individual sandstone beds may have resulted from lateral migration and abandonment of channels and bars or from changes in streamflow velocities during deposition (e.g., Miall, 1977; Uba et al., 2005). Mudstones are interpreted to represent overbank deposition in adjacent floodplain settings that were later subjected to incision by sandy channel systems (Miall, 1977).

Lithofacies Association 2: Cross-Stratified Sandstone with Interbedded Conglomerate

This lithofacies association occurs within the intermediate ~500-m-thick section of the Peñas Formation and is composed primarily of medium- to coarse-grained sandstones with trace granules to cobbles (Table 2). Individual sandstone beds vary in thickness from medium to very thickly bedded (~0.1–1.5 m) and extend laterally for tens to a few hundred meters (Fig. 5B). Amalgamated channel-fill structures with low-angle cross stratification are common in this facies association, suggesting multistory channels, possibly in a distributary system (Fig. 5C). Interbedded with the sandstones are clast-supported, subrounded to well-rounded granule to cobble conglomerates that typically define internally stratified lenses that are not laterally extensive. Mudstone is limited in this facies association and occurs as discontinuous lenses.

Deposition of this facies association is interpreted to have occurred in the intermediate zone of a streamflow-dominated alluvial fan system, with most deposition taking place in sandy and gravelly channels (e.g., Miall, 1985, 1996; Hampton and Horton, 2007). Most sand was deposited in amalgamated channel systems in which individual channels were <1.5 m thick. Horizontally and trough cross-stratified conglomerate lenses are interpreted as gravel deposited in longitudinal bars or lag deposits (e.g., Miall, 1985). The limited occurrence of overbank sediments and absence of debris flow deposits suggests a depositional environment situated in the channel-dominated intermediate portion of an alluvial fan, downslope of any proximal region affected by sediment gravity flows and upslope of the distal region characterized by mixed floodplain and channel environments.

Lithofacies Association 3: Conglomerate and Interbedded Cross-Stratified Sandstone

This lithofacies association defines the upper ~200 m of the Peñas Formation and is distinguished by a larger average grain size (Table 2). This lithofacies association is composed of clast-supported, moderately sorted, pebble to cobble conglomerates displaying imbrication of subrounded to rounded clasts and erosive

Downloaded from gsabulletin.gsapubs.org on July 6, 2010

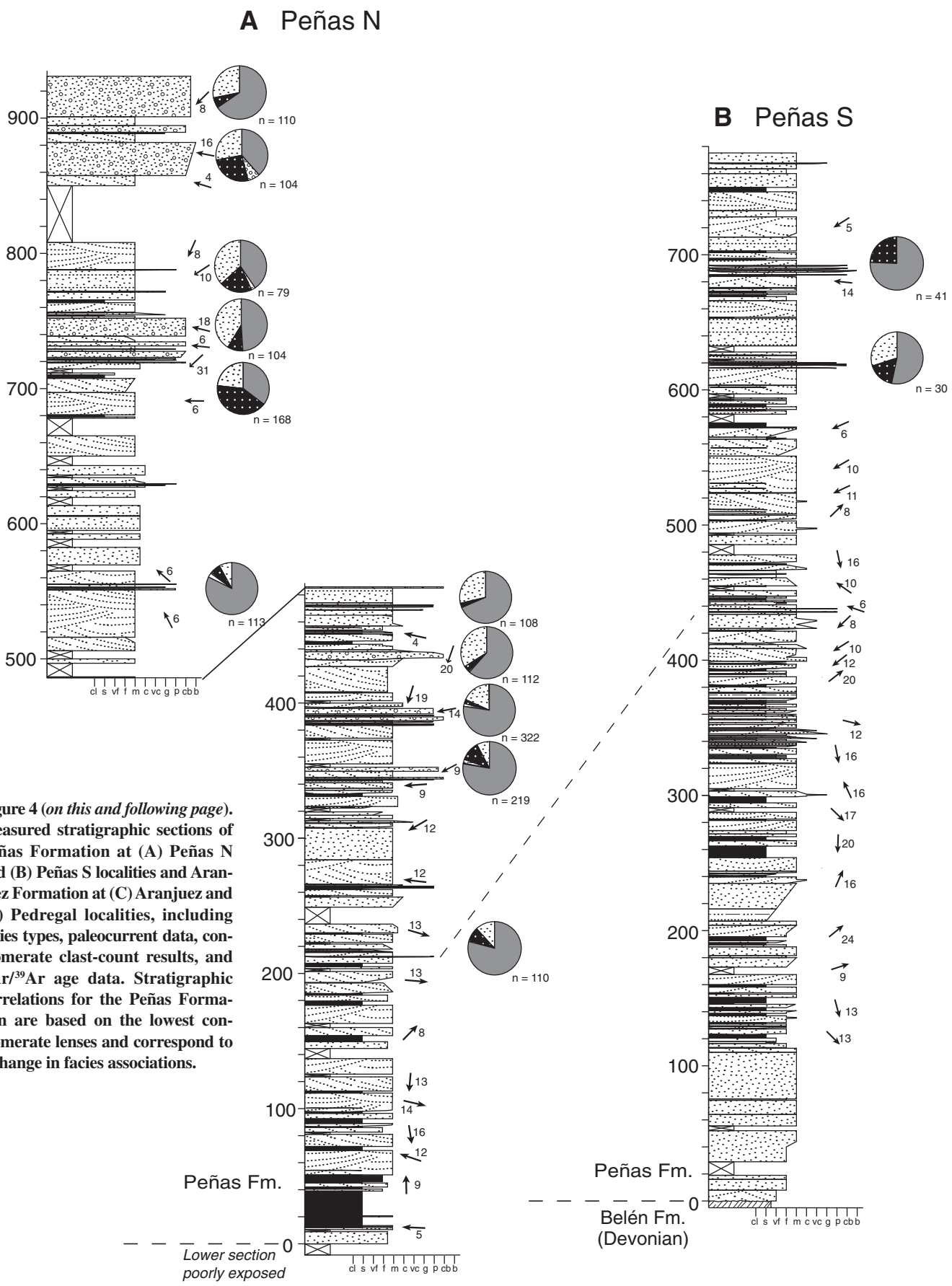

Figure 4 (*on this and following page*). Measured stratigraphic sections of Peñas Formation at (A) Peñas N and (B) Peñas S localities and Aranjuez Formation at (C) Aranjuez and (D) Pedregal localities, including facies types, paleocurrent data, conglomerate clast-count results, and $^{40}Ar/^{39}Ar$ age data. Stratigraphic correlations for the Peñas Formation are based on the lowest conglomerate lenses and correspond to a change in facies associations.

Downloaded from gsabulletin.gsapubs.org on July 6, 2010

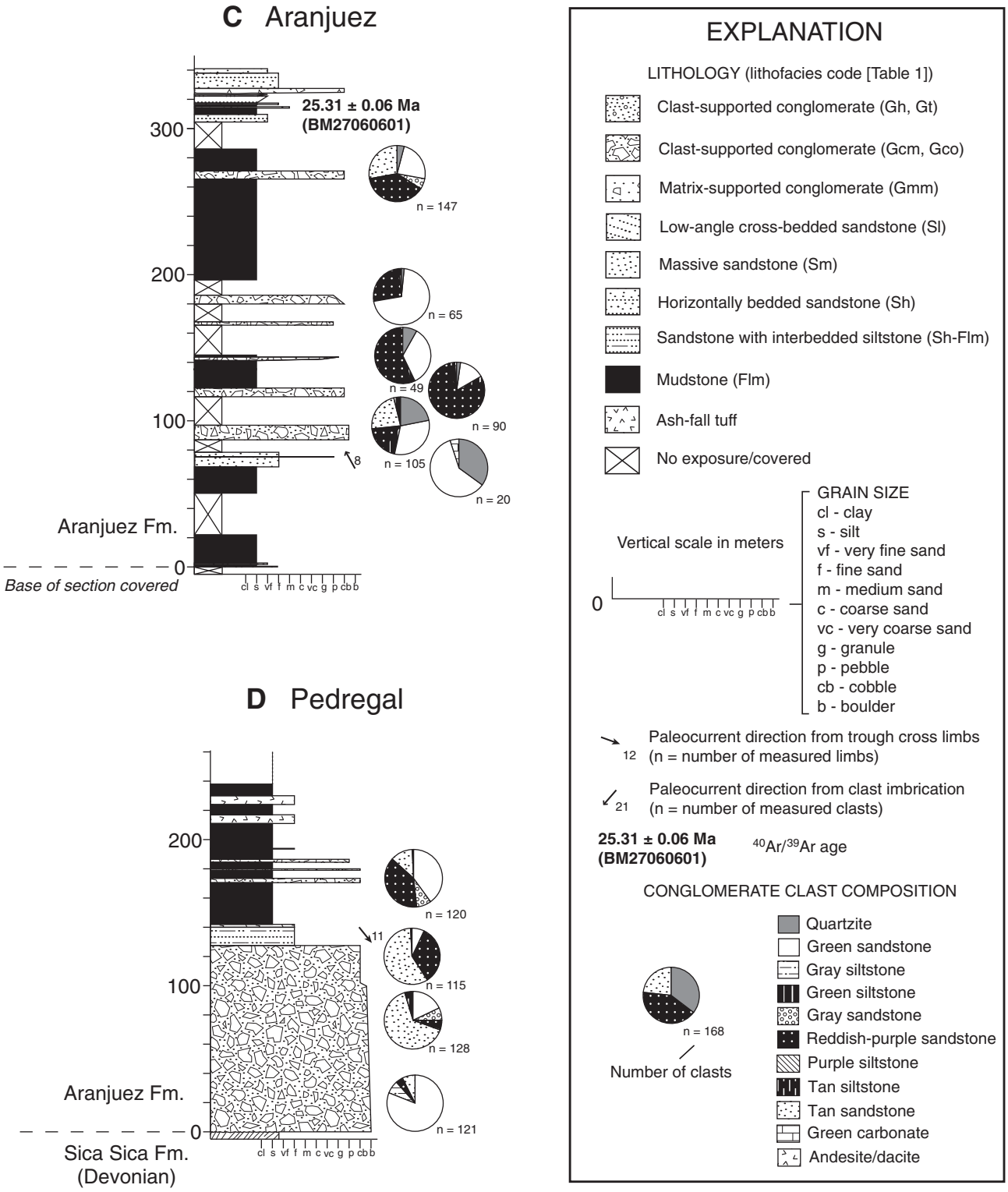

Figure 4 (*continued*).

Downloaded from gsabulletin.gsapubs.org on July 6, 2010

TABLE 1. DESCRIPTION AND INTERPRETATION OF SEDIMENTARY LITHOFACIES (AFTER MIALL, 1985; UBA ET AL., 2005)

Facies code	Description	Interpretation
Gcm	Clast-supported, massive conglomerate. Poorly sorted, subrounded to angular, none to very poorly developed normal to inverse grading, pebbles to boulders.	Clast-rich debris flows
Gco	Clast-supported, organized conglomerate. Poorly sorted, subrounded to angular. Normal grading, pebbles to boulders.	Traction bedload
Gmm	Matrix-supported, massive conglomerate. Poorly sorted, subrounded to angular. No grading, pebbles to cobbles.	Plastic debris flows
Gh	Clast-supported, crudely horizontally stratified conglomerate. Moderately sorted, well rounded to subrounded. Granules to cobbles with imbrications.	Longitudinal bedforms, lag deposits
Gt	Clast-supported, trough cross-stratified conglomerate. Moderately sorted, well rounded to subrounded, pebbles to boulders.	Minor channel fills, transverse bars
Sl	Low-angle (<15°) cross-stratified sandstone. Very fine to coarse-grained, trace pebbles. Moderately to well sorted.	Channel fills, crevasse splays, dune migration
Sh	Horizontally laminated sandstone. Very fine- to medium-grained, trace cobbles and pebbles. Moderately to well sorted.	Planar bed flow, upper flow regime
Sm	Massive sandstone. Fine- to coarse-grained, trace cobbles and pebbles. Moderately to well sorted.	Hyperconcentrated sediment-gravity flows
Ss	Sandstone with basal scour surface. Very coarse to medium-grained, trace granules. Normal grading.	Erosive channel fills
Flm	Massive or laminated siltstone to claystone.	Overbank, abandoned channel or suspension deposits

basal contacts (Fig. 5D). Individual conglomerate beds are up to 0.5 m thick and persist laterally for tens of meters. Interbedded with the conglomerates are medium- to coarse-grained sandstones with trace pebbles and cobbles. Sandstone beds are medium to very thickly bedded (~0.2 to >2 m) and extend laterally for tens to a few hundred meters.

This facies association is interpreted as the result of deposition in shallow gravelly channels in the proximal zone of an alluvial fan system (e.g., Miall, 1985; Miall, 1996; Hampton and Horton, 2007). The clast-supported conglomerates generally exhibit lenticular geometries and erosive basal contacts consistent with deposition in shallow channels of low sinuosity (e.g., Miall, 1985). More poorly organized, clast-supported conglomerates and massive (structureless) sandstone beds may suggest a limited amount of hyperconcentrated sediment gravity flows. The absence of overbank mudstones and diminished occurrence of sandstone channels are consistent with a proximal depositional environment upslope of the distal region that is characterized by greater sand and mud deposition in mixed channel and floodplain settings.

Aranjuez Formation

Two stratigraphic sections were measured in the >340-m-thick Aranjuez Formation (Figs. 3C, 4C, and 4D). The base of the Aranjuez Formation lies in angular unconformity above the Devonian Sica Sica Formation and younger, subhorizontal middle Miocene–Pliocene La Paz Formation unconformably overlaps tilted beds of the Aranjuez Formation. The facies association of this formation represents deposition in a mass-flow–dominated alluvial fan (Table 2).

Lithofacies Association 4: Conglomerate and Interbedded Sandstone and Mudstone

The Aranjuez Formation consists primarily of poorly sorted, massive, disorganized conglomerates (Fig. 6A) interbedded with massive to poorly stratified pebbly sandstones and sandy mudstones (Fig. 6B and Table 2). Individual conglomerate beds are clast- or matrix-supported, have lenticular to sheet-like geometries, and are laterally extensive for tens of meters. Mudstone and sandstone beds are massive to thinly bedded and typically contain very fine grained sand- to pebble-rich lenses that are laterally continuous for several meters to tens of meters. Some sandstone and mudstone sections contain primary to slightly reworked ash-fall tuffs up to 6 m thick that display sharp, nonerosive basal contacts (Fig. 6C).

This facies association represents deposition by high-energy sediment and fluid gravity flows in the medial to proximal zone of a mass-flow–dominated alluvial fan (e.g., Blair and McPherson, 1994). Disorganized, clast- and matrix-supported conglomerates are interpreted as the products of clast-rich and plastic debris flows, respectively, with minor massive sandstones representing hyperconcentrated sediment-gravity flows. The more organized, clast-supported conglomerate facies represents traction bedload sedimentation during waning sheet floods in poorly confined channels (e.g., Blair and McPherson, 1994). Mudstones to fine-grained sandstones are interpreted as deposits in interchannel overbank flow regions (e.g., Miall, 1985; Blair and McPherson, 1994) that were capable of preserving primary to slightly reworked ash-fall tuffs.

Depositional Synthesis

On the basis of the observed sedimentary lithofacies (Table 1; Figs. 5 and 6), the Peñas Formation is considered to represent deposition

TABLE 2. LITHOFACIES ASSOCIATIONS AND RELATED LITHOFACIES

Facies association	Lithofacies	Thickness (m)	Characteristics	Interpretation
1: Cross-stratified sandstone and interbedded mudstone	Sl, Ss, Sh, Sm, Flm	~425	Moderately to well-sorted, fine- to medium-grained sandstones, tan to orange; interbedded dark-red siltstones	Deposition in sandy channel systems and muddy overbank settings of the distal zone of a streamflow-dominated alluvial fan or a moderate-energy, sandy braided fluvial system
2: Cross-stratified sandstone and interbedded conglomerate	Sl, Sh, Sm, Gh, Gt, Flm	~500	Moderately sorted, medium- to coarse-grained sandstones, white to red, with trace granules to cobbles; interbedded clast-supported granule to cobble conglomerate lenses up to ~1 m thick, subrounded to rounded, clast imbrication; trace mudstone lenses	Deposition in sandy and gravelly channel systems, with limited muddy overbanks in the intermediate zone of a streamflow-dominated alluvial fan
3: Conglomerate and interbedded cross-stratified sandstone	Gh, Gt, Sm, Sh, Sl	~200	Moderately sorted, clast-supported pebble to cobble conglomerates, subrounded to rounded, clast imbrication, erosive basal contacts; interbedded moderately sorted, medium- to coarse-grained sandstones, white to red, with trace pebbles and cobbles	Deposition in shallow gravelly channel systems in the proximal zone of a streamflow-dominated alluvial fan
4: Conglomerate and interbedded sandstone and mudstone	Gcm, Gco, Gmm, Sh, Sm, Flm	>340	Poorly sorted, massive, disorganized conglomerates, subrounded to angular, clast or matrix supported, may have very poorly developed normal or inverse grading; interbedded massive to thinly bedded pebbly sandstones, sandy mudstones, and very thinly to thinly bedded fine-grained sandstones, tan to purple	High-energy, sediment and fluid gravity debris flows in the intermediate to proximal zone of a mass-flow–dominated alluvial fan

Downloaded from gsabulletin.gsapubs.org on July 6, 2010

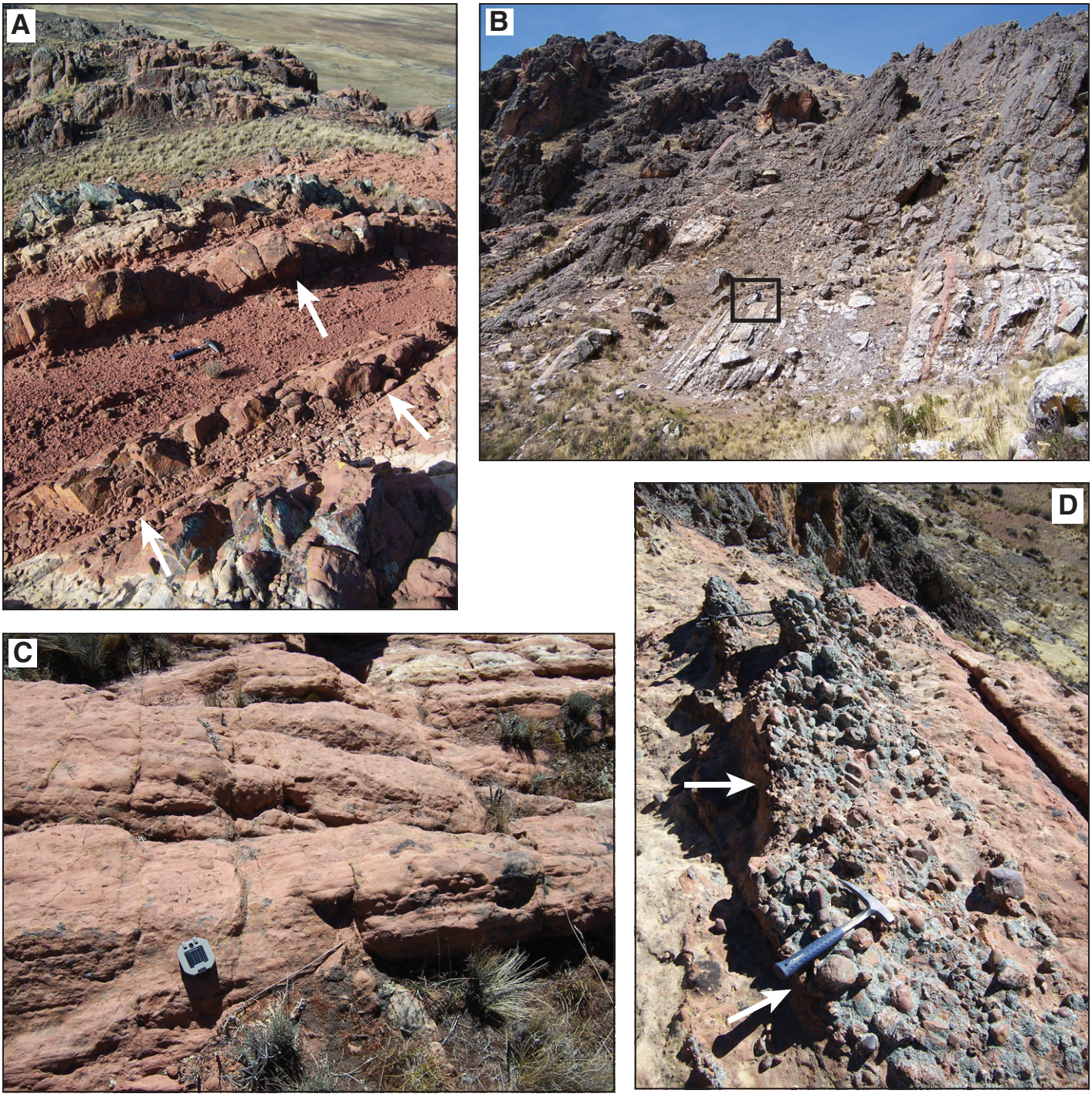

Figure 5. Photographs of representative lithofacies in the Peñas Formation. (A) Interbedded sandstone and mudstone of lithofacies association 1, representing deposition in the distal zone of a streamflow-dominated alluvial fan or braided fluvial system. Roughly downdip view includes sandstones with basal scour surfaces (Ss) cutting into underlying mudstone (Flm) in center of photo and sandstone (Sl) in base of photo (arrows). Rock hammer for scale. (B) Representative exposure of medium to very thickly bedded, lateral continuous sandstone of lithofacies association 2, interpreted as deposition in an intermediate zone of a streamflow-dominated alluvial fan. Seated person (outlined) for scale. (C) Stacked lenticular channel geometries observed in low-angle cross-stratified sandstone (Sl) of the intermediate zone of a streamflow-dominated alluvial fan (lithofacies association 2). Compass for scale. (D) Trough cross-stratified cobble conglomerate (Gt) displaying channel-fill geometry and erosive base (arrows), and interbedded sandstone (Sm, Sh) in lithofacies association 3, representing deposition in the proximal zone of a streamflow-dominated alluvial fan. Rock hammer for scale.

Downloaded from gsabulletin.gsapubs.org on July 6, 2010

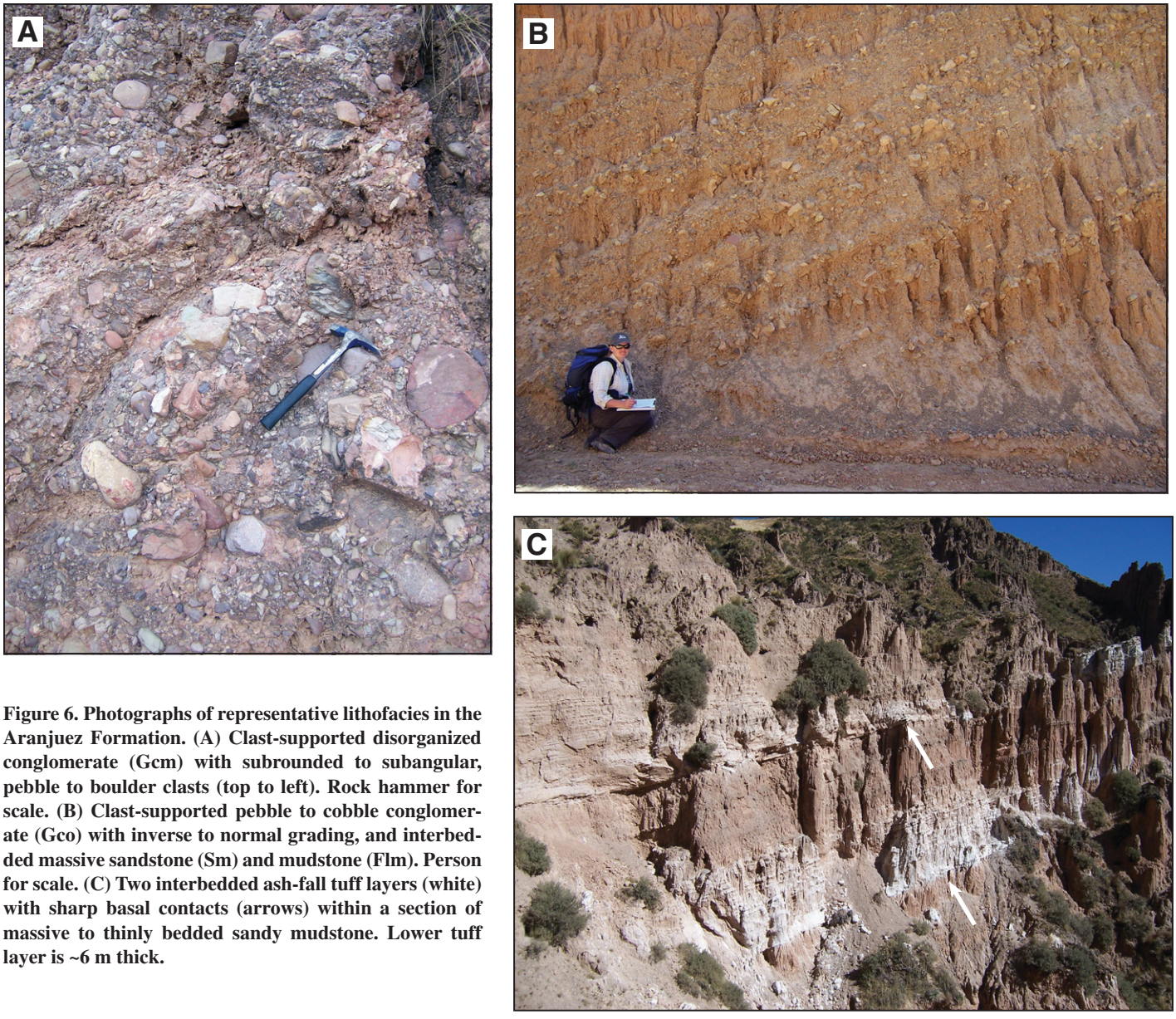

Figure 6. Photographs of representative lithofacies in the Aranjuez Formation. (A) Clast-supported disorganized conglomerate (Gcm) with subrounded to subangular, pebble to boulder clasts (top to left). Rock hammer for scale. (B) Clast-supported pebble to cobble conglomerate (Gco) with inverse to normal grading, and interbedded massive sandstone (Sm) and mudstone (Flm). Person for scale. (C) Two interbedded ash-fall tuff layers (white) with sharp basal contacts (arrows) within a section of massive to thinly bedded sandy mudstone. Lower tuff layer is ~6 m thick.

in a streamflow-dominated alluvial fan (Table 2) that may have constituted part of a terminal fan system (e.g., Friend, 1978; Nichols, 1987; Kelly and Olsen, 1993; Ridgway and DeCelles, 1993; Newell et al., 1999; Smith, 2000) adjacent to a braided fluvial system farther downslope. A terminal fan commonly contains a fan-shaped, distributary network of fluvial channels in an arid to semiarid environment where water infiltrates and evaporates before escaping the system by surface flow (Friend, 1978; Nichols, 1987; Kelly and Olsen, 1993; Newell et al., 1999). Terminal fans tend to be sand dominated and have a lower gradient in comparison to typical coarse-grained alluvial fans (Kelly and Olsen, 1993). Terminal fans also generally exhibit confined flow in proximal environments that pass downslope into a distal region of unconfined flow (Kelly and Olsen, 1993; Hampton and Horton, 2007). The apparent absence of major fluvial systems downslope of the alluvial fan facies associations in the Peñas Formation may suggest a terminal fan setting, partially analogous to fluvial megafans of the modern foreland basin adjacent to the central Andes (e.g., Horton and DeCelles, 2001; Leier et al., 2005; Uba et al., 2005).

The three lithofacies associations of the Peñas Formation can be distinguished from each other on the basis of grain sizes and sedimentary lithofacies (Table 2). The proximal zone of the streamflow-dominated alluvial fan (lithofacies association 3) contains predominantly conglomerate and is distinguished by a channelized pebble to cobble conglomerate facies (Fig. 5D) and an absence of mudstone facies. In comparison, channelized sandstone with thin granule to pebble conglomerate lenses (Figs. 5B and 5C) are the typical signatures of the medial zone of the streamflow-dominated alluvial fan (lithofacies association 2). Both the medial and proximal zones of the streamflow-dominated alluvial fan lithofacies associations are distinguishable from either a distal alluvial fan or braided fluvial environment (lithofacies association 1). Whereas the proximal and medial lithofacies associations include substantial conglomerate lithofacies, the distal lithofacies association is composed

Downloaded from gsabulletin.gsapubs.org on July 6, 2010

of only medium-grained sandstone to siltstone (Fig. 5A). Additionally, the distal alluvial fan lithofacies association contains thick units (up to 18 m) of floodplain mudstone, whereas mudstone is limited to absent in the medial and proximal zones of the alluvial fan lithofacies associations. The Aranjuez Formation is interpreted to represent deposition in the medial to proximal zones of a mass-flow–dominated alluvial fan (e.g., Blair and McPherson, 1994). Deposits of coarse-grained debris flows and related lithofacies in a distributary pattern characterize mass-flow–dominated alluvial fans (Blair and McPherson, 1994; Miall, 1996). The mass-flow–dominated alluvial fan facies association of the Aranjuez Formation can be distinguished from the streamflow-dominated alluvial fan lithofacies associations of the Peñas Formation by differences in types of lithofacies, grain size, and degree of clast roundness. Whereas the Aranjuez Formation includes disorganized matrix-supported conglomerates (Fig. 6A) diagnostic of debris flows, lithofacies of the Peñas Formation include stratified, channelized conglomerates and sandstones with interbedded overbank mudstones indicative of streamflow processes. Additionally, the conglomerates of the Aranjuez Formation contain angular to subrounded pebble to boulder clasts, whereas conglomerates of the Peñas Formation consist of well rounded to subrounded pebbles to cobbles.

DEPOSITIONAL AGE CONSTRAINTS

New $^{40}Ar/^{39}Ar$ results for an igneous unit from the lowermost exposed basin fill and interbedded ash-fall tuffs provide constraints on the depositional age of the Peñas and Aranjuez formations in the northeastern Altiplano (Table 3 and GSA Data Repository Table DR1)[1]. $^{40}Ar/^{39}Ar$ laser total-fusion analyses were performed at the New Mexico Geochronology Research Laboratory on a collection of individual sanidine crystals separated from eight samples. For each sample, weighted mean ages and 2σ errors are calculated on the basis of $^{40}Ar/^{39}Ar$ results for 9 to 25 individual sanidine crystals (Fig. 7 and Table 3).

The $^{40}Ar/^{39}Ar$ ages for the eight samples in this study range from late Oligocene to middle Miocene. In the Jankho Khaua region (Fig. 2), five samples (samples BM29060601–BM29060605) from a hypabyssal trachyte sill and pyroclastic flow contained within a steeply dipping section of the Aranjuez Formation (Matos, 2002) yield nearly indistinguishable weighted mean ages ranging from a maximum age of 27.42 ± 0.09 Ma to a minimum age of 27.31 ± 0.07 Ma (Figs. 7A–7E; Table 3). An ash-fall tuff (sample BM27060601) from near the top of the measured section of the Aranjuez Formation (Figs. 3C and 4) has a weighted mean age of 25.31 ± 0.06 Ma (Fig. 7F and Table 3). A tuff (sample 6061402) from the lowest section of the Peñas Formation exposed at Cerro Santa Ana (Fig. 3B) has an identical weighted mean age, within error, of 25.29 ± 0.04 Ma (Fig. 7G and Table 3). The youngest dated tuff (sample BM28060601), from the unconformably overlying La Paz Formation (Fig. 3C), has a weighted mean age of 14.11 ± 0.07 Ma (Fig. 7H and Table 3).

TABLE 3. SUMMARY OF $^{40}AR/^{39}AR$ RESULTS

Sample	Formation (locality)	Lithology	n	MSWD	Age (Ma)	±2σ (Ma)
BM29060605	Aranjuez Fm. (Jankho Khaua)	Trachyte sill	13	1.8	27.42	0.09
BM29060602	Aranjuez Fm. (Jankho Khaua)	Pyroclastic flow	14	1.0	27.41	0.06
BM29060601	Aranjuez Fm. (Jankho Khaua)	Trachyte sill	9	1.5	27.40	0.06
BM29060603	Aranjuez Fm. (Jankho Khaua)	Trachyte sill	9	1.0	27.34	0.07
BM29060604	Aranjuez Fm. (Jankho Khaua)	Pyroclastic flow	9	0.8	27.31	0.07
BM27060601	Aranjuez Fm. (Aranjuez)	Tuff	15	1.1	25.31	0.06
6061402	Peñas Fm. (Cerro Santa Ana)	Tuff	25	1.1	25.29	0.04
BM28060601	La Paz Fm. (Zona Sur)	Tuff	12	0.6	14.11	0.07

Note: n—number of sanidine grains analyzed; MSWD—mean square of weighted deviates.

These new $^{40}Ar/^{39}Ar$ age results are generally consistent with $^{40}Ar/^{39}Ar$ step-heating results for biotite grains obtained by Gillis et al. (2006) from reworked tuffs and tuff clasts in the Aranjuez Formation, which have late Oligocene ages ranging from 27.4 ± 1.1 Ma to 25.1 ± 1.1 Ma (2σ). Gillis et al. (2006) also reported a single early Oligocene age of 33.1 ± 1.6 Ma (their sample Taa06) for the Aranjuez Formation. However, this sample of reworked tuff is located only ~40 m downsection of a sample yielding an age of 26.7 Ma ± 1.1 Ma (Gillis et al., 2004), which would suggest an anomalously low accumulation rate (<10 m/Myr) within the Altiplano hinterland, where Cenozoic accumulation rates commonly exceed 500 m/Myr (Horton et al., 2001; Hampton and Horton, 2007). Given this contradiction, the sample's relatively higher age errors, and the reworked nature of the tuff, we regard the early Oligocene $^{40}Ar/^{39}Ar$ age for this sample as an estimate of the maximum possible depositional age for the Aranjuez Formation, with the late Oligocene representing the principal age of Aranjuez deposition.

Based on the $^{40}Ar/^{39}Ar$ results presented here and by Gillis et al. (2006), deposition of the Peñas and Aranjuez formations was clearly ongoing during the late Oligocene, with the principal depositional ages ranging from ~27.5 Ma to ~25 Ma. Because the lowest exposed stratigraphic levels in the east (~27.4 Ma age for lowermost exposed Aranjuez Formation) are ~2 Myr older than the lowest levels in the west (~25.3 Ma age for the lowermost exposed Peñas Formation), we infer a general west-southwestward migration of the locus of basin subsidence, comparable in size and scale to the progradation of the alluvial fan depositional systems toward the Altiplano. Moreover, growth structures (discussed below) observed in the Aranjuez Formation indicate that shortening was contemporaneous with sedimentation in the Altiplano at this time.

SYNDEPOSITIONAL AND POSTDEPOSITIONAL STRUCTURES

Structural relationships observed in the Peñas and Aranjuez formations suggest that shortening occurred both during and after their deposition. Both the Peñas and Aranjuez formations are exposed in steeply dipping panels in close proximity to west-southwest–directed thrust faults of the central Andean backthrust belt (Figs. 2 and 3). In most localities, the formations occur in the footwalls of thrust faults that are, in turn, carried in the hanging wall of additional thrust faults farther to the west-southwest, notably the Huarina thrust (Fig. 2). In this structural setting, the Peñas and Aranjuez formations were subjected to significant postdepositional deformation. For example, a moderate to high degree of internal deformation involving small-scale folding and intraformational thrust faulting affected the Aranjuez succession (Fig. 8A) in the vicinity of the tuff dated at 25.31 ± 0.06 Ma (Fig. 7F and Table 3). However, the unconformably overlying middle to upper Miocene La Paz Formation, including a tuff-bearing section yielding an age of 14.11 ± 0.07 Ma (Fig. 7H and Table 3), has undergone little to no deformation. These relationships indicate that postdepositional deformation affecting the Aranjuez and Peñas formations occurred during the late Oligocene to early Miocene, likely between ~25 Ma and 15 Ma.

In addition to postdepositional structures, evidence of growth strata suggests syndepositional shortening was active during late Oligocene deposition of the Aranjuez and Peñas formations. Although not observed in the Peñas Formation, potentially due to insufficient exposure, the

[1]GSA Data Repository item 2010105, $^{40}Ar/^{39}Ar$ analytical methods results (Table DR1), and summary of recalculated modal point-count data for sandstones (Table DR2), is available at http://www.geosociety.org/pubs/ft2010.htm or by request to editing@geosociety.org.

Downloaded from gsabulletin.gsapubs.org on July 6, 2010

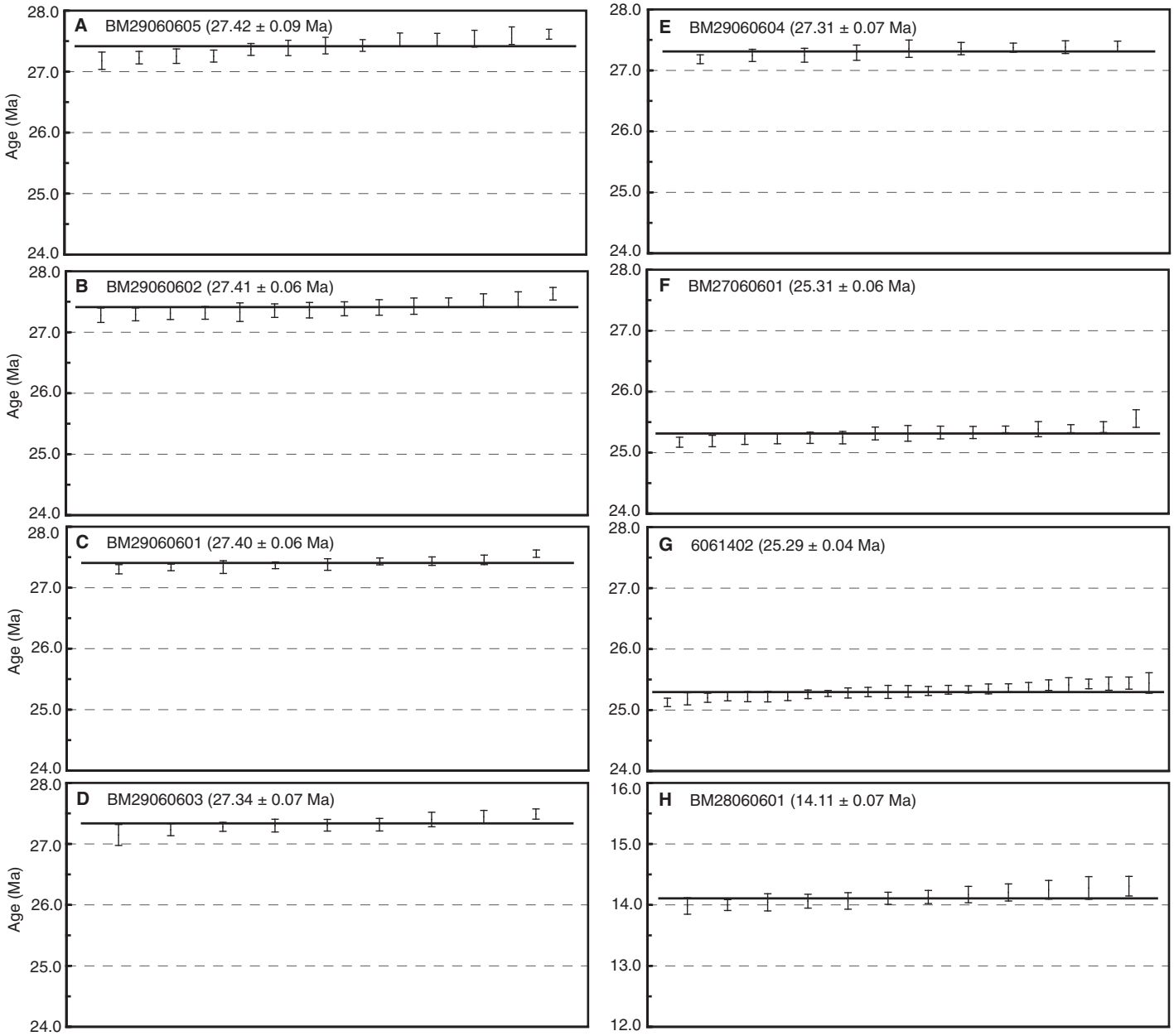

Figure 7. Plots depicting laser total-fusion $^{40}Ar/^{39}Ar$ ages for individual sanidine crystals from eight samples (A–H). In each plot, the horizontal line represents the calculated weighted mean age (2σ) for each sample. Vertical lines represent 1σ error bars for individual crystal ages. (A–E) Samples BM29060601–BM29060605: igneous unit containing hypabyssal trachyte sill and pyroclastic flow in lowermost Aranjuez Formation, near Jankho Khaua (Fig. 2). (F) Sample BM27060601: tuff from uppermost Aranjuez Formation (Figs. 3C and 4). (G) Sample 6061402: tuff from lowest exposed Peñas Formation at Cerro Santa Ana (Fig. 3B). (H) Sample BM28060601: tuff from the La Paz Formation that unconformably overlies the Aranjuez Formation (Fig. 3C). See Table DR1 [see footnote 1] for individual $^{40}Ar/^{39}Ar$ age analyses.

Aranjuez Formation displays several indicators of structural growth during sedimentation. Along the Rio Khellkata river-cut exposures east of Rio La Paz (Fig. 8B), fanning bedding dips, abrupt lateral thickness variations, and internal angular unconformities are observed in the Aranjuez Formation. The presence of these growth structures suggests that shortening was partially contemporaneous with late Oligocene deposition of the Aranjuez Formation at ~27.5 Ma to 25 Ma, although shortening likely persisted into early Miocene time. Although there is no direct evidence for the precise onset of deformation in the study area, it is conceivable that local shortening commenced prior to late Oligocene deposition of the Aranjuez Formation.

SEDIMENT PROVENANCE

Sediment Dispersal Patterns

Paleocurrent measurements were collected from the Peñas and Aranjuez formations from trough-cross limbs in sandstone and conglomerates (method I of DeCelles et al., 1983) and

Downloaded from gsabulletin.gsapubs.org on July 6, 2010

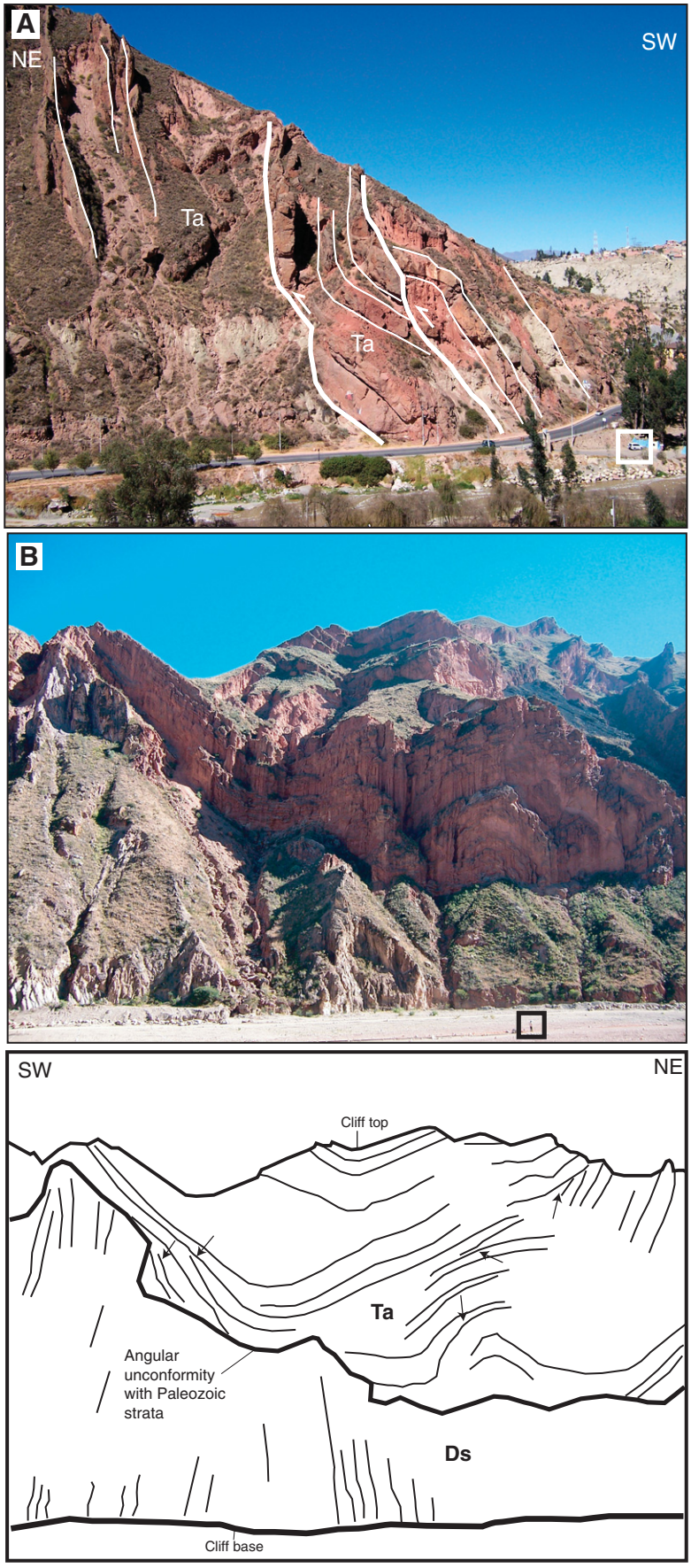

Figure 8. (A) Photograph of intraformational thrust faults and mesoscopic folds in exposures of the Aranjuez Formation near Zona Sur (south La Paz), indicating significant postdepositional deformation. Vehicles (outlined) and road for scale. (B) Photograph and line drawing of growth strata developed in the Aranjuez Formation (Ta) in angular unconformity above the Devonian Sica Sica Formation (Ds) in Rio Khellkata river-cut exposures east of Rio La Paz (Fig. 2). Fanning bedding dips, abrupt lateral thickness variations, and internal angular unconformities (arrows) attest to syndepositional deformation. Person (outlined) in foreground is ~100 m in front of cliff face.

from conglomerate clast imbrication (Fig. 4). Paleocurrent indicators for the measured sections of the Peñas Formation show a change in the average flow direction with stratigraphic level (Fig. 9). The paleocurrent indicators in the lower ~425 m of the Peñas Formation show a wide range of flow directions, with the average flow toward the southeast (Fig. 9A). The paleocurrent directions in the upper part of the Peñas section (~425–1100 m) indicate predominantly west-southwest–directed flow with a moderately divergent dispersal pattern (Fig. 9B). A general westward flow direction is also measured in outcrops of the Peñas Formation at Cerro Santa Ana (Fig. 3B). The upsection change in sediment dispersal is considered to be the result of initial flow potentially parallel to an uplifted source region followed by transverse flow approximately perpendicular to the source region. This pattern is consistent with the facies interpretations suggesting that deposition in the medial to proximal zones of a streamflow-dominated terminal fan prograded over more distal deposits of a distal fan to braided fluvial system. In other words, the temporal shift in depositional systems may coincide with the upsection replacement of southeastward, potentially axial flow by west-directed flow in diverging distributary channels of the medial to proximal fan. For the Aranjuez Formation, paleocurrent measurements from this study and Gillis et al. (2006) indicate an average south-southwest-directed paleoflow in a variable to poorly defined divergent pattern (Fig. 9C). Although the paleocurrent patterns are not definitive, the facies associations and average flow directions for the Aranjuez Formation suggest deposition in an alluvial fan system derived from the east-northeast.

Downloaded from gsabulletin.gsapubs.org on July 6, 2010

Compositional Methods

To determine the provenance of the Peñas and Aranjuez formations and possible stratigraphic trends, conglomerate and sandstone compositional data were collected from the four measured stratigraphic sections and additional isolated outcrops. Conglomerate clast counts were conducted on the outcrop in 28 localities at an approximate stratigraphic spacing of 20–60 m and consisted of lithologic identification of an average of 100 clasts per count. Although many conglomerate clasts cannot be identified at the formation level with confidence, some clast types may be attributed to specific rock units or specific intervals of the Paleozoic stratigraphic section. In the Altiplano, granite and gneiss clasts are typically derived from Precambrian basement that may have been exposed in the Western Cordillera or from Permo-Triassic granites in the Eastern Cordillera (Horton et al., 2002). Quartzite clasts are commonly associated with the Ordovician Amutara Formation, and carbonate clasts are likely derived from either the Carboniferous Copacabana Formation or the Upper Cretaceous El Molino Formation (e.g., Sempere, 1995; Suárez and Diaz, 1996; McQuarrie and DeCelles, 2001; Horton et al., 2002; Gillis et al., 2006). Several types of sandstone clasts may be derived from Silurian–Devonian strata: Silurian sandstones are generally gray to green (e.g., Catavi Formation); Devonian sandstones are typically reddish purple (e.g., Vila Vila Formation) and tan (e.g., Sica Sica and Colpacucho formations) (Suárez and Diaz, 1996).

Compositional data for 39 fine- to coarse-grained sandstones were determined for samples collected from measured sections at an ~50 m interval. For each sample, a standard petrographic thin section was cut, etched with concentrated hydrofluoric acid, and stained for potassium feldspar. Four-hundred points per thin section were analyzed using a modified Gazzi-Dickinson method of point counting to determine composition (e.g., Gazzi, 1966; Dickinson, 1970; Ingersoll et al., 1984; Dickinson, 1985). Framework grains (>0.0625 mm) were classified using the petrographic counting parameters listed in Table 4. In cases of diagenetic alteration, such as partial alteration of feldspar to clay minerals, framework grains were counted as the original grain type. Lithic fragments mainly consist of metamorphic grains, argillaceous grains, and polycrystalline quartz grains. Another common framework grain is monocrystalline quartz with rounded syntaxial overgrowths. Matrix, authigenic cement, and pore spaces were also included in the point-counting parameters. Recalculated detrital modal percentages (Table DR2 [see footnote 1]) for quartz-feldspar-lithic fragments (Q-F-L %), monocrystalline quartz-feldspar-total lithic fragments (Qm-F-Lt %), and metamorphic-volcanic-sedimentary lithic fragments (Lm-Lv-Ls %) are based on methods defined by Ingersoll et al. (1984) and Dickinson (1985).

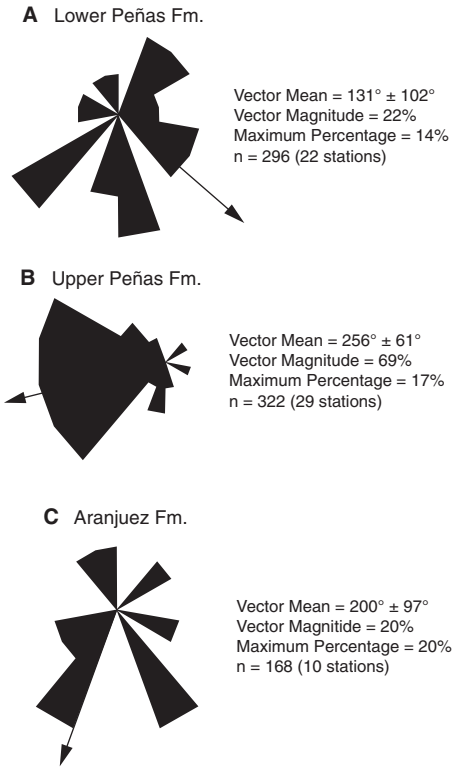

Figure 9. Paleocurrent data for measured sections of the Peñas and Aranjuez formations displaying vector mean and standard deviation, vector magnitude, maximum percentage, and number of measurements for each rose diagram. (A) Lower Peñas Formation (0 to ~425 m). (B) Upper Peñas Formation (~425–1100 m). (C) Combined paleocurrent data from this study and Gillis et al. (2006) for the Aranjuez Formation.

Peñas Formation

Description

Clastic provenance of the Peñas Formation was determined from 16 conglomerate clast counts (Fig. 10) and 34 sandstone point counts (Fig. 11) for the measured sections. Overall, the dominant conglomerate clasts are quartzite, reddish-purple sandstone, and tan sandstone, with minor amounts of gray siltstone, gray sandstone, and green sandstone (Figs. 4A, 4B, and 10A). Granite and gneiss clasts were not observed, and volcanic clasts are extremely rare. Similar clast compositions were observed in two conglomerate clast counts at Cerro Santa Ana (Figs. 3B and 10B). Individual clast counts of conglomerates in the Peñas N section generally display an upsection decrease in the relative abundance of quartzite clasts, accompanied by an increase in reddish-purple and tan sandstone clasts (Fig. 4A).

Compositionally, sandstones of the Peñas Formation are sublitharenites and quartz arenites, reflecting their high percentage of monocrystalline quartz, limited lithic fragments, and lack of feldspar (e.g., Pettijohn et al., 1987). The compositions do not vary significantly upsection or between stratigraphic sections, with average Q-F-L % = 91-1-8 and average Qm-F-Lt % = 88-1-11 (Fig. 11A and Table DR2 [see footnote 1]). No samples display pressure solution textures common in highly compacted sandstone, and the interstitial space is predominantly occupied with infiltrated mud or epimatrix (e.g.,

TABLE 4. PARAMETERS FOR SANDSTONE POINT COUNTS

Symbol	Grain categories	Recalculated parameters
Qmm	Monocrystalline quartz	Q-F-L:
Qmo	Monocrystalline quartz with rounded syntaxial overgrowths	Q = Qmm + Qmo + Qp + Qpt
Qp	Polycrystalline quartz	F = Fp + Fk
Qpt	Polycrystalline quartz with tectonite fabric	L = Lv + Ls + Lm
Fp	Plagioclase feldspar	
Fk	Potassium feldspar	Qm-F-Lt:
Lvv	Vitric volcanic-hypabyssal lithic fragments	Qm = Qmm + Qmo
Lvf	Felsitic volcanic-hypabyssal lithic fragments	F = Fp + Fk
Lvm	Microlitic volcanic-hypabyssal lithic fragments	Lt = Lv + Ls + Lm + Qp + Qpt
Lvl	Lathwork volcanic-hypabyssal lithic fragments	
Lmv	Metavolcanic lithic fragments	Lm-Lv-Ls:
Lmm	Polycrystalline mica lithic fragments	Lm = Lmv + Lmm + Lmt + Lma
Lmt	Quartz-feldspar-mica tectonite lithic fragments, including phyllite	Lv = Lvv + Lvf + Lvm + Lvl
Lma	Quartz-feldspar-mica aggregate lithic fragments	Ls = Lss + Lsc
Lss	Argillaceous-shale lithic fragments	
Lsc	Extra-basinal carbonate lithic fragments	
M	Monocrystalline mica	
D	Dense minerals (pyroxenes, amphiboles, etc.)	
Misc.	Miscellaneous and unidentified grains	
M/C	Matrix (<0.0625 mm) and/or cement	
Pore	Pore space	

Downloaded from gsabulletin.gsapubs.org on July 6, 2010

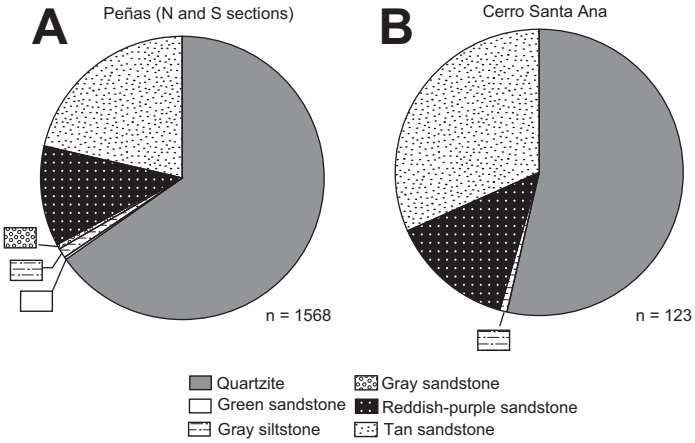

Figure 10. Conglomerate clast compositional data for the Peñas Formation. (A) Total compositional data for measured sections of the Peñas Formation. See Figure 3A for locations and Figure 4 for individual clast counts. (B) Total compositional data for outcrops of the Peñas Formation at Cerro Santa Ana. See Figure 3B for locations and individual clast counts.

Dickinson, 1970). Most monocrystalline quartz grains display straight extinction, but some display undulatory and wavy extinction, with a few grains exhibiting strain lamellae. Some monocrystalline quartz grains exhibit rounded syntaxial overgrowths, suggesting erosion of quartz-cemented sandstone. Polycrystalline quartz with tectonite fabric is also present in the samples. Feldspar is rare in the sandstone samples; where present, potassium feldspar is more abundant than plagioclase. The dominant lithic fragments consist of metamorphic quartz-feldspar-mica tectonites and aggregates and sedimentary argillaceous-shale fragments, with trace felsitic volcanic lithic fragments (Fig. 11B). In both measured sections, the proportion of sedimentary lithic fragments increases upsection (Fig. 11B).

Interpretation

Based on conglomerate clast compositions (Fig. 10), sandstone petrofacies (Fig. 11), and west-directed paleoflow direction (Fig. 9), the Peñas Formation was likely derived from recycling of quartz-rich Paleozoic metasedimentary and sedimentary rocks of the Eastern Cordillera. The average sandstone Qm-F-Lt % plots in the "recycled-orogenic" tectonic setting of Dickinson (1985); however, the sedimentary facies associations indicate a first- to second-order alluvial sampling, which is not ideal to use with the third-order tectonic settings of the Dickinson Qm-F-Lt ternary diagram (e.g., Ingersoll, 1990; Ingersoll et al., 1993). On the other hand, "recycled-orogenic" settings tend to produce uniform compositions at all sampling scales (Ingersoll et al., 1993). The recycled provenance of these sandstones is verified by the dominance of metamorphic and sedimentary lithic fragments, and limited degree of volcanic detritus (e.g., Ingersoll, 1990). The presence of monocrystalline quartz with rounded syntaxial overgrowths, polycrystalline quartz grains with tectonite fabrics, and quartz-feldspar-mica tectonites (Fig. 11) is consistent with derivation from quartz-cemented sandstone, quartzite, and phyllite found in Paleozoic strata of the Eastern Cordillera. Additionally, polycrystalline quartz and monocrystalline quartz with undulatory extinction observed in these samples suggests that these grains were likely derived from a low-grade metamorphic source (Basu, 1985). The trace amounts of felsitic volcanic lithic grains could be the erosional products of either Cenozoic volcanic rocks related to arc magmatism or Jurassic–Cretaceous hypabyssal intrusions and flows exposed locally in the Eastern Cordillera (e.g., Kennan et al., 1995; SERGEOMIN, 1997; DeCelles and Horton, 2003; Jiménez and López-Velásquez, 2008).

Conglomerate clast compositions (Fig. 10) are consistent with sandstone compositions, and suggest derivation from Paleozoic rocks of the Eastern Cordillera. The dominant clast lithology observed in the Peñas Formation is white to dark-gray quartzite, which is attributed to the Ordovician Amutara Formation. Reddish-purple and tan sandstone clasts were likely derived from the Devonian Vila Vila and Sica Sica formations, respectively. Limited clasts of gray siltstone, green sandstone, and gray sandstone may have been derived from the Silurian Uncia and Catavi formations. The lack of granite and gneiss clasts indicates that

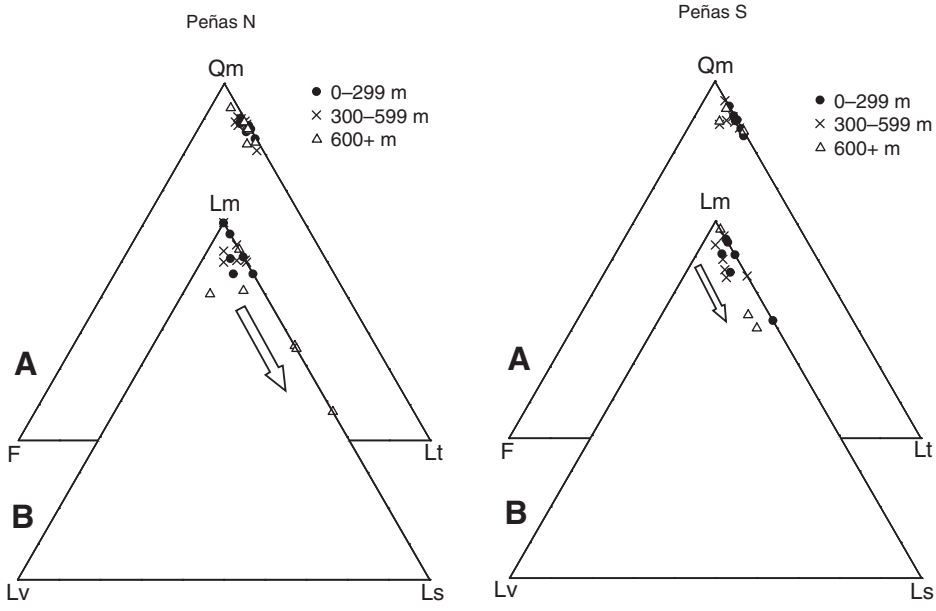

Figure 11. (A) Monocrystalline quartz-feldspar-total lithic fragments (Qm-F-Lt) and (B) metamorphic-volcanic-sedimentary lithic fragments (Lm-Lv-Ls) ternary diagrams for 34 sandstone samples of the Peñas Formation collected from the Peñas N (left) and Peñas S (right) measured sections (Fig. 4). Note the upsection trends (arrows) toward greater sedimentary lithic fragments. Recalculated modal percentages for samples are shown in Table DR2 [see footnote 1].

Downloaded from gsabulletin.gsapubs.org on July 6, 2010

sediments were not derived from Precambrian basement in the Western Cordillera. Additionally, the lack of granite clasts implies that the abundant Permo-Triassic granites exposed today in the Eastern Cordillera were not exhumed during deposition of the Peñas Formation. The lack of carbonate clasts suggests that the Copacabana and El Molino formations were not exposed over significant areas of the source region.

The proportion of lithic fragment types found within the Peñas Formation sandstones changes upsection from predominantly metamorphic to roughly equal metamorphic and sedimentary fragments, suggesting that the source-rock composition evolved through time from primarily metasedimentary to mixed sedimentary and metasedimentary (Fig. 11B). The compositional trend in conglomerate clast types is consistent with the sandstone petrographic data, showing an upsection reduction in Ordovician quartzite and increase in younger Devonian sandstone (Figs. 4A and 4B).

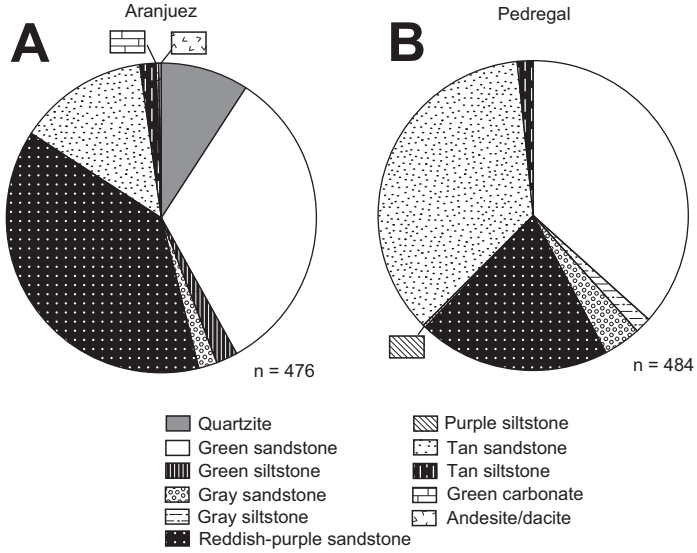

Figure 12. Conglomerate clast compositional data for the Aranjuez Formation. See Figure 3C for locations and Figure 4 for individual clast counts. (A) Total compositional data for the Aranjuez measured section. (B) Total compositional data for the Pedregal measured section.

Aranjuez Formation

Description

Ten conglomerate clast counts and five sandstone point counts provide provenance information for the Aranjuez Formation. Reddish-purple sandstone, green sandstone, and tan sandstone are the dominant clast types, with gray sandstone, gray siltstone, and tan siltstone representing minor components (Fig. 12). Clasts of quartzite and green siltstone with trace amounts of green carbonate and andesite-dacite are only observed in the Aranjuez section. Gneiss and granite clasts are absent from these conglomerates. Individual clast counts show a poorly defined compositional trend of decreasing quartzite clasts upsection in the Aranjuez measured section (Fig. 4C), and an upsection decrease in green sandstone accompanied by increased tan and reddish-purple sandstone in the lower 120 m of the Pedregal measured section (Fig. 4D).

Sandstone facies are relatively uncommon in the conglomerate- and mudstone-dominated Aranjuez Formation. The sandstones are typically very fine to fine grained and are classified as lithic wackes based on their quartz- and lithic-rich, feldspar-poor composition and high percentage of silt (<0.0625 mm) matrix of infiltrated mud and calcite cement (e.g., Pettijohn et al., 1987). The modal composition of the Aranjuez sandstone samples is variable, with average Q-F-L % = 64-4-32 and average Qm-F-Lt % = 61-4-35 (Fig. 13A and Table DR2 [see footnote 1]). Most monocrystalline quartz grains display straight extinction, with a small percentage showing undulatory and wavy extinction. Polycrystalline quartz and monocrystalline quartz with rounded syntaxial overgrowths are less common framework constituents. The sandstone samples contain limited feldspar, with potassium feldspar more common than plagioclase. Lithic fragments are mostly metamorphic quartz-feldspar-mica tectonites and aggregates, with lesser amounts of sedimentary argillaceous-shale and felsitic volcanic fragments (Fig. 13B). No clear stratigraphic trends in sandstone composition are recognized for the Aranjuez Formation.

Interpretation

Similar to the Peñas Formation, the combination of conglomerate clast compositions (Fig. 12), sandstone petrofacies (Fig. 13), and westward-directed paleoflow directions indicate that the Aranjuez Formation was likely derived from erosion of Paleozoic strata in the Eastern Cordillera. The predominantly metamorphic to sedimentary lithic-rich compositions of these first-order sandstone samples (Fig. 13) suggest provenance from a recycled mixed metasedimentary-sedimentary source (e.g., Ingersoll, 1990; Ingersoll et al., 1993). The relatively small amount of polycrystalline quartz indicates that the majority of quartz grains were subjected to high strain prior to erosion (e.g., Basu, 1985). Monocrystalline quartz grains with rounded syntaxial overgrowths derived from eroded quartz-cemented sandstone also supports the interpretation of primarily sedimentary rocks in the source region.

Conglomerate clast compositions suggest erosion of Silurian to Devonian strata, with limited Ordovician and Carboniferous provenance (Fig. 12). Green to gray sandstone and gray to green siltstone clasts were likely eroded from Silurian Catavi and Uncia formations, respectively. The eroded Devonian strata are represented by clasts of reddish-purple sandstone (Vila Vila Formation), tan sandstone (Sica Sica Formation), and tan siltstone (Belén Formation). Quartzite clasts in the Aranjuez section were likely derived from the Ordovician Amutara Formation, with green carbonate clasts possibly representing minor input from the Carboniferous Copacabana Formation or Upper Cretaceous El Molino Formation. Granite clasts are absent, indicating that the Permo-Triassic granites in the Eastern Cordillera had not yet reached the surface during deposition of the Aranjuez Formation, and that sediments were not derived from Precambrian basement exposed in the Western Cordillera.

Similar to the Peñas Formation, upsection trends of decreasing quartzite clasts in the Aranjuez measured section and decreasing green sandstone clasts accompanied by increasing tan and reddish-purple sandstone clasts in the lower Pedregal measured section suggest relatively increased detrital input from younger stratigraphic units with time. Although the Peñas and Aranjuez formations are age-equivalent (Table 3), there is a difference in clast compositions expressed as a greater proportion of quartzite clasts in the Peñas Formation (Figs. 10 and 12).

Downloaded from gsabulletin.gsapubs.org on July 6, 2010

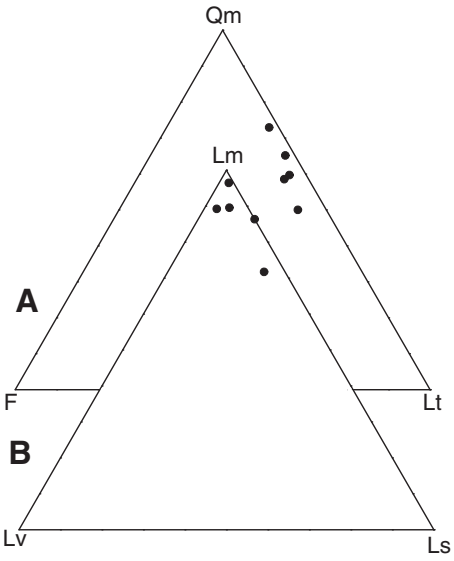

Figure 13. (A) Monocrystalline quartz-feldspar-total lithic fragments (Qm-F-Lt) and (B) metamorphic-volcanic-sedimentary lithic fragments (Lm-Lv-Ls) ternary diagrams for five sandstone samples of the Aranjuez Formation collected from the Aranjuez and Pedregal measured sections (Fig. 4). Recalculated modal percentages for samples are shown in Table DR2 [see footnote 1].

This compositional difference potentially represents along-strike variations in source rock exposure within the Eastern Cordillera. At face value, the clast compositions of the Peñas and Aranjuez formations suggest that late Oligocene rock uplift in the Eastern Cordillera was not regionally uniform, with deeper (Ordovician) stratigraphic levels exposed in the north adjacent to the Peñas Formation, but principally younger (Silurian) levels exposed farther south. Despite these compositional variations, both the Peñas and Aranjuez formations show consistent upsection trends toward increased input from relatively younger Paleozoic strata, suggestive of broadly similar unroofing patterns in comparable structural systems.

DISCUSSION

Basin Provenance

The sedimentology, provenance, and $^{40}Ar/^{39}Ar$ ages for the Peñas and Aranjuez formations suggest late Oligocene–early Miocene deposition in a west-southwestward prograding system of streamflow- and mass-flow–dominated alluvial fans composed of sediments derived from the Eastern Cordillera. The Peñas Formation displays an upward coarsening trend (Fig. 4), with conglomerates absent in the lower portion but dominant near the top. This pattern is interpreted as an increase in the proximity of the sediment source to the basin with time. The observed facies associations reflect this temporal change in source-area proximity, with an upsection facies transition from distal fan or braided fluvial deposition to proximal, streamflow-dominated fan deposition.

Provenance data from conglomerate clast counts (Figs. 4, 10, and 12) reveal an increase in the amount of sediments derived from younger Paleozoic strata with time. For example, the lower Peñas Formation was primarily derived from Ordovician rocks, but detrital compositions upsection represent roughly equal contributions from Ordovician and Devonian rocks (Figs. 4A and 4B). The Aranjuez Formation also reflects this trend, with an upsection reduction in Ordovician and Silurian detritus relative to Devonian detritus (Figs. 4C and 4D). A similar trend is expressed in the sandstone petrographic data by an upsection shift in the ratio of sedimentary to metamorphic lithic fragments (Fig. 11B). These upsection provenance shifts seem counterintuitive because simple erosional unroofing of a single fault block would be expected to produce an upsection trend in which detritus is systematically older and from lower structural levels.

Several possibilities may explain this provenance trend, including shifts in drainage networks within an evolving sediment source area, erosion through a single thrust sheet, or erosion of newly uplifted exposures of younger Paleozoic strata. In the first case, changes within the source drainage network may have focused erosion in areas with Devonian strata, resulting in an increased proportion of younger sedimentary fragments. In the second case, erosion through a single thrust sheet could produce an initial influx of Ordovician quartzite derived from the hanging wall followed by an increased amount of footwall-derived Devonian detritus. Although plausible, neither of these two options can explain the temporal increase in grain size represented by the upward coarsening trend in the basin. Therefore, we favor a third explanation in which erosion of progressively younger Paleozoic strata is the product of a systematic advance of fold-thrust deformation toward the basin, with the activation of new thrust faults in greater proximity to the basin.

Structural Evolution

We propose that the mechanisms responsible for the observed sedimentological and provenance trends in the Peñas and Aranjuez formations are related to west-southwestward growth of the central Andean backthrust belt concurrent with sedimentation (Fig. 14). In this scenario, prior to and during earliest basin development, thrust-induced denudation in the Eastern Cordillera resulted in unroofing of Ordovician strata (Fig. 14A). Forward propagation of west-southwest–directed thrust faults during Peñas and Aranjuez deposition increased the proximity of the sediment source to the basin (Fig. 14B), uplifting younger (Devonian) strata that resulted in an increase in average grain size and erosion of these younger rocks. Eventually, continued advance of the central Andean backthrust belt resulted in fault propagation to the west-southwest of the basin (Fig. 14C), initiating deposition of younger synorogenic sedimentary strata (e.g., Coniri Formation; Sempere et al., 1990; Horton et al., 2002) and hanging-wall uplift and deformation of the Peñas and Aranjuez deposits. This interpretation (Fig. 14) accounts for both the sedimentological trend toward more proximal facies and the provenance trend in which younger Paleozoic rocks were introduced into the sediment source area. Additionally, this interpretation is supported by the west-southwestward migration of the locus of basin subsidence inferred from our new $^{40}Ar/^{39}Ar$ ages for the basin fill (Table 3).

Previous studies have attributed growth of the central Andean backthrust belt to emplacement of an eastward-propagating basement megathrust over a 12 km ramp located near the eastern Altiplano–Eastern Cordillera boundary (McQuarrie and DeCelles, 2001; McQuarrie, 2002; McQuarrie et al., 2008). Continued tectonic wedging on this basement megathrust allowed slip to be transferred to the overlying Paleozoic strata along décollement horizons located in the Ordovician and Silurian formations, resulting in growth of the west-southwest–directed backthrust belt (McQuarrie, 2002; McQuarrie et al., 2008). However, the precise sequence of deformation within that backthrust belt has been difficult to unravel (e.g., Gillis et al., 2006). The stratigraphic and provenance relationships observed within the Peñas and Aranjuez formations are consistent with a model of systematic forward propagation of sequential thrust faults to the west-southwest (Fig. 14). This "in sequence" model of thrusting and advance of the central Andean backthrust belt toward the Altiplano may help explain the partial discrepancy between previously reported evidence for rapid exhumation that is derived from thermochronology compared to that derived from basin analysis.

Exhumational Record

Thermochronological studies in the Eastern Cordillera suggest that a period of rapid cooling associated with rock uplift initiated during the middle Eocene at ~40 Ma and continued

Downloaded from gsabulletin.gsapubs.org on July 6, 2010

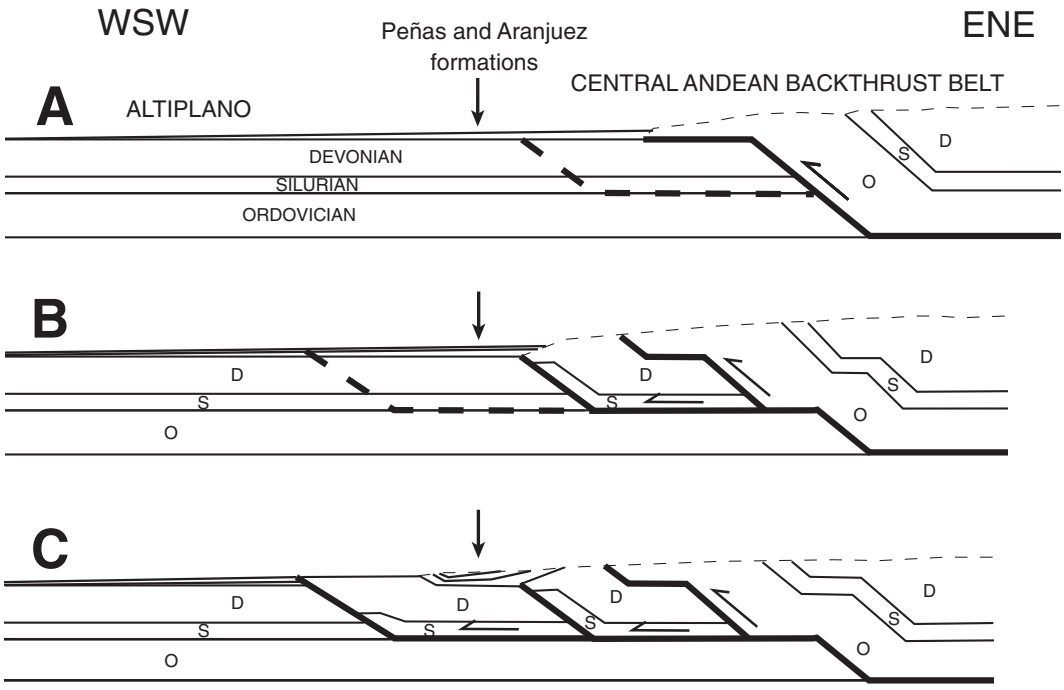

Figure 14. Schematic cross sections depicting a simplified sequence of fold-thrust deformation in the central Andean backthrust belt during late Oligocene to early Miocene basin development (Peñas and Aranjuez formations). Vertical arrow indicates location of measured sections with time. Approximate décollement horizons are based on balanced cross sections by McQuarrie (2002), McQuarrie et al. (2008), and field observations. (A) Early deformation in the backthrust belt resulting in uplift and erosion of Silurian–Devonian strata, followed by exposure of Ordovician rocks, which dominated initial provenance in the basin. (B) West-southwestward propagation of thrust front into the Altiplano causing uplift of previously flat-lying Paleozoic strata and increasing the proximity of the source area, resulting in increases in average grain size and amount of Devonian-derived detritus. (C) Continued advance of thrust front inducing postdepositional deformation of the Peñas and Aranjuez formations and initiation of younger synorogenic sedimentation farther to the west-southwest.

until ~25 Ma (Benjamin et al., 1987; McBride et al., 1987; Farrar et al., 1988; Masek et al., 1994; Barnes et al., 2006; Gillis et al., 2006; Ege et al., 2007; Barnes et al., 2008; McQuarrie et al., 2008). Provenance data from this study document the presence of Ordovician quartzite clasts in the lower Peñas Formation, which indicates that lower Paleozoic metasedimentary rocks in the Eastern Cordillera were subjected to erosion during the late Oligocene (Figs. 10, 12, and 14A). This implies that considerable exhumation and erosion of portions of the Eastern Cordillera occurred prior to the deposition of the east-derived deposits in the Altiplano, possibly during an initial, middle Eocene to early Oligocene period of uplift-related rapid cooling. However, exhumation was likely insufficient to expose the Eastern Cordillera's Permo-Triassic granites by the late Oligocene, because no granite clasts are observed in the Peñas and Aranjuez formations. Although there are no clear erosional products from the early phase of exhumation affecting the Paleozoic section, one possibility is that the initial erosional products may have been deposited in wedge-top basins closer to the core of the central Andean backthrust belt and were subsequently uplifted and eroded during migration of the deformation front toward the Altiplano. Given the sequential west-southwestward advance of the central Andean backthrust belt, it seems likely that a temporal delay would be observed between the onset of rapid exhumation in the core of the backthrust belt, notably the Cordillera Real, and the frontal zones of the backthrust belt along the margins of the Altiplano. Therefore, thermochronological evidence supporting the proposed middle Eocene onset of rapid cooling by uplift in the Cordillera Real (Gillis et al., 2006) should not be considered to be in conflict with the late Oligocene influx of locally derived sediment in intermontane or hinterland basins (MacFadden et al., 1985; Sempere et al., 1990; Horton et al., 2002; this study) at the leading (west-southwestern) edge of the central Andean backthrust belt.

Regional Implications

Growth structures, stratigraphic trends, and $^{40}Ar/^{39}Ar$ ages for the Peñas and Aranjuez formations indicate syndepositional shortening during late Oligocene–early Miocene evolution of a hinterland basin in the northern Altiplano. During this period, much of the eastern Altiplano received an influx of clastic sediments derived from the Eastern Cordillera (MacFadden et al., 1985; Sempere et al., 1990; Horton et al., 2002; Gillis et al., 2004, 2006). Although several possible features may control the kinematic history of fold-thrust deformation, we consider the west-southwestward advance of deformation in the central Andean backthrust belt, away from the core of the Eastern Cordillera, to be the product of substantial crustal thickening within the Eastern Cordillera. Structural evidence also suggests that much of the upper-crustal shortening in the region had terminated in the early Miocene time (McQuarrie and DeCelles, 2001; Horton, 2005; Gillis et al., 2006). Therefore, we propose that concentrated Oligocene–early Miocene shortening within the Eastern Cordillera and eastern Altiplano resulted in sufficient crustal thickening to generate large-scale isostatic uplift and initial expression of the eastern margin of the central Andean plateau.

CONCLUSIONS

(1) Sedimentary lithofacies and facies associations identified in the upper Oligocene to lower Miocene Peñas and Aranjuez formations of the northern Altiplano of Bolivia indicate nonmarine deposition of coarse clastic sediment within the central Andean backthrust belt. Accumulation took place in the proximal, medial, and distal zones of a streamflow-dominated terminal fan system, in a mass-flow–dominated alluvial fan, and potentially in braided fluvial environments at the downslope margins of the fans. Upsection transitions to more proximal facies are consistent with west-southwestward

Downloaded from gsabulletin.gsapubs.org on July 6, 2010

progradation of depositional systems and increased proximity to the sediment source areas in the Eastern Cordillera.

(2) $^{40}Ar/^{39}Ar$ ages for igneous units within the lowermost exposed Aranjeuz Formation and interbedded ash-fall tuffs within the Aranjuez, Peñas, and overlying La Paz formations provide key temporal constraints on the onset of basin evolution, rate of basin advance, and timing of upper-crustal shortening in the central Andean backthrust belt. $^{40}Ar/^{39}Ar$ ages in the Aranjuez and Peñas formations range from ~27.5 Ma to 25 Ma, indicating consistent late Oligocene accumulation. Deposition of the overlying La Paz Formation commenced in middle Miocene time. The $^{40}Ar/^{39}Ar$ ages from the lowermost exposed strata in different localities show that initial Aranjuez deposition in proximal settings predated initial Peñas deposition in distal settings by ~2 Myr, indicative of a west-southwestward migration of the locus of basin subsidence. Growth strata and stratal overlap relationships demonstrate that motion along fold-thrust structures of the central Andean backthrust belt was contemporaneous with late Oligocene to early Miocene deposition of the Aranjuez and Peñas formations, but had ceased prior to middle Miocene deposition of the La Paz Formation.

(3) Sediment provenance information derived from conglomerate clast compositions, sandstone petrographic data, and paleocurrent orientations show that Paleozoic sedimentary and metasedimentary rocks of the Eastern Cordillera were the principal sediment sources for the Peñas and Aranjuez formations of the northern Altiplano. The compositional provenance data reveal a complex unroofing pattern in which an upsection increase in younger detritus is expressed by an increased proportion of Devonian clasts relative to Ordovician clasts and by an increase in the ratio of sedimentary to metasedimentary lithic fragments. These provenance trends require the introduction of younger rocks in the source area and, therefore, are not compatible with simple unroofing of a single fault block.

(4) The complex upsection shift in provenance and general west-southwestward progradation of depositional systems can be attributed to sequential activation of fold-thrust structures within the central Andean backthrust belt. Advance of upper-crustal shortening toward the leading (west-southwestern) edge of the backthrust belt provides a mechanism for both the increased proximity of sediment source areas and the introduction of younger Paleozoic detritus from more-frontal thrust sheets. At a regional scale, a long-term west-southwestward shift in deformation could explain the ~10–15 Myr discrepancy between the estimated middle Eocene (~40 Ma) onset of rapid exhumation inferred from thermochronological studies and the late Oligocene influx of sediment in the Altiplano.

(5) The Peñas and Aranjuez formations in the northern Altiplano are among the best exposed records of the middle Cenozoic influx of east-derived sediments within a regional hinterland basin. This period of basin accumulation was coeval with a significant period of Oligocene–early Miocene shortening in the central Andean backthrust belt. Advance of the deformation front along the Altiplano–Eastern Cordillera boundary further suggests large-scale crustal thickening, and by inference, isostatic uplift and initial topographic growth of the eastern margin of the central Andean plateau.

ACKNOWLEDGMENTS

This research was partially supported by National Science Foundation grants EAR-0510441 and EAR-0908518 and a graduate student research grant from the Geological Society of America. We thank Néstor Jiménez, Sohrab Tawackoli, Robert Gillis, Raymond Ingersoll, Andrew Leier, Jesse Mosolf, and Nadine McQuarrie for beneficial discussions. Dana Roeber Murray and Nelsón Ayala provided assistance in the field. Constructive reviews by Jason Covault, Andrew Hanson, Abhijit Basu, and Charles Mitchell helped improve the manuscript.

REFERENCES CITED

Allmendinger, R.W., Jordan, T.E., Kay, S.M., and Isacks, B.L., 1997, The evolution of the Altiplano-Puna plateau of the central Andes: Annual Review of Earth and Planetary Sciences, v. 25, p. 139–174, doi: 10.1146/annurev.earth.25.1.139.

Barnes, J.B., Ehlers, T.A., McQuarrie, N., and Pelletier, J.D., 2006, Variations in Eocene to recent erosion across the central Andean fold-thrust belt, northern Bolivia: Implications for plateau evolution: Earth and Planetary Science Letters, v. 248, p. 118–133, doi: 10.1016/j.epsl.2006.05.018.

Barnes, J.B., Ehlers, T.A., McQuarrie, N., O'Sullivan, P.B., and Tawackoli, S., 2008, Thermochronometer record of central Andean Plateau growth, Bolivia (19.5°S): Tectonics, v. 27, doi: 10.1029/2007TC002174.

Basu, A., 1985, Reading provenance from detrital quartz, *in* Zuffa, G.G., ed., Provenance of Arenites: Dordrecht, D. Reidel, p. 231–247.

Beck, S.L., Zandt, G., Myers, S.C., Wallace, T.C., Silver, P.G., and Drake, L., 1996, Crustal thickness variations in the Central Andes: Geology, v. 24, p. 407–410, doi: 10.1130/0091-7613(1996)024<0407:CTVITC>2.3.CO;2.

Benjamin, M.T., Johnson, N.M., and Naeser, C.W., 1987, Recent rapid uplift in the Bolivian Andes: Evidence from fission-track dating: Geology, v. 15, p. 680–683, doi: 10.1130/0091-7613(1987)15<680:RRUITB>2.0.CO;2.

Blair, T.C., and McPherson, J.G., 1994, Alluvial fans and their natural distinction from rivers based on morphology, hydraulic processes, sedimentary processes, and facies assemblages: Journal of Sedimentary Research, v. A64, p. 450–489.

DeCelles, P.G., and Giles, K.N., 1996, Foreland basin systems: Basin Research, v. 8, p. 105–123, doi: 10.1046/j.1365-2117.1996.01491.x.

DeCelles, P.G., and Horton, B.K., 2003, Early to middle Tertiary foreland basin development and the history of Andean crustal shortening in Bolivia: Geological Society of America Bulletin, v. 115, p. 58–77, doi: 10.1130/0016-7606(2003)115<0058:ETMTFB>2.0.CO;2.

DeCelles, P.G., Langford, R.P., and Schwartz, R.K., 1983, Two new methods of paleocurrent determination from trough cross-stratification: Journal of Sedimentary Petrology, v. 53, p. 629–642.

Dickinson, W.R., 1970, Interpreting detrital modes of graywacke and arkose: Journal of Sedimentary Petrology, v. 40, p. 695–707.

Dickinson, W.R., 1985, Interpreting provenance relations from detrital modes of sandstones, *in* Zuffa, G.G., ed., Provenance of Arenites: Dordrecht, D. Reidel, p. 333–361.

Ege, H., Sobel, E.R., Scheuber, E., and Jacobshagen, V., 2007, Exhumation history of the southern Altiplano plateau (southern Bolivia) constrained by apatite fission track thermochronology: Tectonics, v. 26, p. TC1004, doi: 10.1029/2005TC001869.

Farrar, E., Clark, A.H., Kontak, D.J., and Archibald, D.A., 1988, Zongo-San Gabon zone: Eocene foreland boundary of central Andean orogen, northwest Bolivia and southeast Peru: Geology, v. 16, p. 55–58, doi: 10.1130/0091-7613(1988)016<0055:ZSGNZE>2.3.CO;2.

Friend, P.F., 1978, Distinctive features of some ancient river systems, *in* Miall, A.D., ed., Fluvial Sedimentology: Canadian Society of Petroleum Geologists Memoir no. 5, p. 531–542.

Garzione, C.N., Molnar, P., Libarkin, J.C., and MacFadden, B.J., 2006, Rapid late Miocene rise of the Bolivian Altiplano: Evidence for removal of mantle lithosphere: Earth and Planetary Science Letters, v. 241, p. 543–556, doi: 10.1016/j.epsl.2005.11.026.

Garzione, C.N., Hoke, G.D., Libarkin, J.C., Withers, S., MacFadden, B., Eiler, J., Ghosh, P., and Mulch, A., 2008, Rise of the Andes: Science, v. 320, p. 1304–1307, doi: 10.1126/science.1148615.

Gazzi, P., 1966, Le arenarie del flysch sopracretaceo dell'Appennino modenese: Correlazioni con il flysch di Monghidoro: Mineralogica et Petrographica Acta, v. 12, p. 69–97.

GEOBOL (Servicio Geológico de Bolivia), 1995a, Carta Geologica de Bolivia, Hoja Achacachi: Servicio Geologico de Bolivia, scale 1:100,000.

GEOBOL (Servicio Geológico de Bolivia), 1995b, Carta Geologica de Bolivia, Hoja de La Paz: Servicio Geologico de Bolivia, scale 1:100,000.

GEOBOL (Servicio Geológico de Bolivia), 1995c, Carta geologica de Bolivia, Hoja Milluni: Servicio Geologico de Bolivia, scale 1:100,000.

Ghosh, P., Garzione, C.N., and Eiler, J.M., 2006, Rapid uplift of the Altiplano revealed through ^{13}C-^{18}O bonds in paleosol carbonates: Science, v. 311, p. 511–515, doi: 10.1126/science.1119365.

Gillis, R.J., Horton, B.K., and Grove, M., 2004, Exhumation history and basin development along the eastern margin of the central Andean plateau, Bolivia: Geological Society of America Abstracts with Programs, v. 36, p. 433.

Gillis, R.J., Horton, B.K., and Grove, M., 2006, Thermochronology, geochronology, and upper crustal structure of the Cordillera Real: Implications for Cenozoic exhumation of the central Andean plateau: Tectonics, v. 25, doi: 10.1029/2005TC001887.

González, M., Diaz-Martinez, E., and Ticlla, L., 1996, Comentarios sobre la estratigrafia del Silurico y Devonico del norte y centro de la Cordillera Oriental y Altiplano de Bolivia: Ponta Grossa, Brazil, Simposio Sul Americano do Siluro-Devoniano, Anais, p. 117–130.

Gubbels, T.L., Isacks, B.L., and Farrar, E., 1993, High-level surfaces, plateau uplift, and foreland development, Bolivian central Andes: Geology, v. 21, p. 695–698, doi: 10.1130/0091-7613(1993)021<0695:HLSPUA>2.3.CO;2.

Hampton, B.A., and Horton, B.K., 2007, Sheetflow fluvial processes in a rapidly subsiding basin, Altiplano plateau, Bolivia: Sedimentology, v. 54, p. 1121–1147, doi: 10.1111/j.1365-3091.2007.00875.x.

Hoke, G.D., and Garzione, C.N., 2008, Paleosurfaces, paleoelevation, and the mechanisms for the late Miocene topographic development of the Altiplano plateau: Earth and Planetary Science Letters, v. 271, p. 192–201, doi: 10.1016/j.epsl.2008.04.008.

Horton, B.K., 1998, Sediment accumulation on top of the Andean orogenic wedge: Oligocene to late Miocene basins of the Eastern Cordillera, southern Bolivia: Geological Society of America Bulletin, v. 110, p. 1174–1192, doi: 10.1130/0016-7606(1998)110<1174:SAOTOT>2.3.CO;2.

Downloaded from gsabulletin.gsapubs.org on July 6, 2010

Horton, B.K., 2005, Revised deformation history of the central Andes: Inferences from Cenozoic foredeep and intermontane basins of the Eastern Cordillera, Bolivia: Tectonics, v. 24, p. TC3011, doi: 10.1029/2003TC001619.

Horton, B.K., and DeCelles, P.G., 1997, The modern foreland basin system adjacent to the Central Andes: Geology, v. 25, p. 895–898, doi: 10.1130/0091-7613(1997)025<0895:TMFBSA>2.3.CO;2.

Horton, B.K., and DeCelles, P.G., 2001, Modern and ancient fluvial megafans in the foreland basin system of the Central Andes, southern Bolivia: Implications for drainage network evolution in fold-thrust belts: Basin Research, v. 13, p. 43–63, doi: 10.1046/j.1365-2117.2001.00137.x.

Horton, B.K., Hampton, B.A., and Waanders, G.L., 2001, Paleogene synorogenic sedimentation in the Altiplano plateau and implications for initial mountain building in the central Andes: Geological Society of America Bulletin, v. 113, p. 1387–1400, doi: 10.1130/0016-7606(2001)113<1387:PSSITA>2.0.CO;2.

Horton, B.K., Hampton, B.A., LaReau, B.N., and Baldellon, E., 2002, Tertiary provenance history of the northern and central Altiplano (central Andes, Bolivia): A detrital record of plateau-margin tectonics: Journal of Sedimentary Research, v. 72, p. 711–726, doi: 10.1306/020702720711.

Ingersoll, R.V., 1990, Actualistic sandstone petrofacies: Discriminating modern and ancient source rocks: Geology, v. 18, p. 733–736, doi: 10.1130/0091-7613(1990)018<0733:ASPDMA>2.3.CO;2.

Ingersoll, R.V., Bullard, T.F., Ford, R.L., Grimm, J.P., Pickle, J.D., and Sares, S.W., 1984, The effect of grain size on detrital modes: A test of the Gazzi-Dickinson point-counting method: Journal of Sedimentary Petrology, v. 54, p. 103–116.

Ingersoll, R.V., Kretchmer, A.G., and Valles, P.K., 1993, The effect of sampling scale on actualistic sandstone petrofacies: Sedimentology, v. 40, p. 937–953, doi: 10.1111/j.1365-3091.1993.tb01370.x.

Isacks, B.L., 1988, Uplift of the central Andean plateau and bending of the Bolivian orocline: Journal of Geophysical Research, v. 93, p. 3211–3231, doi: 10.1029/JB093iB04p03211.

Jiménez, N., and López-Velásquez, S., 2008, Magmatism in the Huarina belt, Bolivia, and its geotectonic implications: Tectonophysics, v. 459, p. 85–106, doi: 10.1016/j.tecto.2007.10.012.

Jiménez De Ríos, G., 1992, Acerca del basamento Precámbrico en el bloque Andino de Bolivia: Sociedad Geológica Boliviana, Boletín (X Congreso Geológico Boliviano, La Paz), v. 27, p. 88–93.

Jordan, T.E., 1995, Retroarc foreland and related basins, *in* Busby, C.J., and Ingersoll, R.V., eds., Tectonics of Sedimentary Basins: Cambridge, Blackwell Science, p. 331–362.

Kelly, S.B., and Olsen, H., 1993, Terminal fans—A review with reference to Devonian examples: Sedimentary Geology, v. 85, p. 339–374, doi: 10.1016/0037-0738(93)90092-J.

Kennan, L., Lamb, S., and Rundle, C., 1995, K-Ar dates from the Altiplano and Cordillera Oriental of Bolivia: Implications for Cenozoic stratigraphy and tectonics: Journal of South American Earth Sciences, v. 8, p. 163–186, doi: 10.1016/0895-9811(95)00003-X.

Lamb, S., and Hoke, L., 1997, Origin of the high plateau in the central Andes, Bolivia, South America: Tectonics, v. 16, p. 623–649, doi: 10.1029/97TC00495.

Lehmann, B., 1978, A Precambrian core sample from the Altiplano/Bolivia: Geologische Rundschau, v. 67, p. 270–278, doi: 10.1007/BF01803266.

Leier, A.L., DeCelles, P.G., and Pelletier, J.D., 2005, Mountains, monsoons, and megafans: Geology, v. 33, p. 289–292, doi: 10.1130/G21228.1.

Lohmann, H.H., 1970, Outline of tectonic history of Bolivian Andes: American Association of Petroleum Geologists Bulletin, v. 54, p. 735–757.

MacFadden, B.J., Campbell, K.E., Ciffelli, R.L., Siles, O., Johnson, N.M., Naeser, C.W., and Zeitler, P.K., 1985, Magnetic polarity stratigraphy and mammalian fauna of the Deseadan (late Oligocene–early Miocene) Salla beds of northern Bolivia: The Journal of Geology, v. 93, p. 223–250, doi: 10.1086/628950.

Masek, J.G., Isacks, B.L., and Fielding, E.L., 1994, Erosion and tectonics at the margins of continental plateaus: Journal of Geophysical Research, v. 99, p. 13,941–13,956, doi: 10.1029/94JB00461.

Matos, R., 2002, Mapeo geológico de La Paz sur, Cordillera Oriental de Bolivia, *in* Argollo, J., ed., Revista Boliviana de Geociencias: La Paz, Bolivia, Universidad Mayor de San Andrés, p. 34–44.

McBride, S.L., Clark, A.H., Farrar, E., and Archibald, D.A., 1987, Delimitation of a cryptic Eocene tectono-thermal domain in the Eastern Cordillera of the Bolivian Andes through K-Ar and ^{40}Ar-^{39}Ar step-heating: Journal of the Geological Society, v. 144, p. 243–255, doi: 10.1144/gsjgs.144.2.0243.

McQuarrie, N., 2002, The kinematic history of the central Andean fold-thrust belt, Bolivia: Implications for building a high plateau: Geological Society of America Bulletin, v. 114, p. 950–963, doi: 10.1130/0016-7606(2002)114<0950:TKHOTC>2.0.CO;2.

McQuarrie, N., and DeCelles, P., 2001, Geometry and structural evolution of the central Andean backthrust belt, Bolivia: Tectonics, v. 20, p. 669–692, doi: 10.1029/2000TC001232.

McQuarrie, N., Horton, B.K., Zandt, G., Beck, S., and DeCelles, P.G., 2005, Lithospheric evolution of the Andean fold-thrust belt, Bolivia, and the origin of the central Andean plateau: Tectonophysics, v. 399, p. 15–37, doi: 10.1016/j.tecto.2004.12.013.

McQuarrie, N., Barnes, J.B., and Ehlers, T.A., 2008, Geometric, kinematic, and erosional history of the central Andean Plateau, Bolivia (15–17°S): Tectonics, v. 27, doi: 10.1029/2006TC002054.

Miall, A.D., 1977, A review of the braided-river depositional environment: Earth-Science Reviews, v. 13, p. 1–62, doi: 10.1016/0012-8252(77)90055-1.

Miall, A.D., 1985, Architectural-element analysis: A new method of facies analysis applied to fluvial deposits: Earth-Science Reviews, v. 22, p. 261–308, doi: 10.1016/0012-8252(85)90001-7.

Miall, A.D., 1996, The Geology of Fluvial Deposits: Berlin, Springer-Verlag, 581 p.

Newell, A.J., Tverdokhlebov, V.P., and Benton, M.J., 1999, Interplay of tectonics and climate on a transverse fluvial system, Upper Permian, Southern Uralian foreland basin, Russia: Sedimentary Geology, v. 127, p. 11–29, doi: 10.1016/S0037-0738(99)00009-3.

Nichols, G.J., 1987, Structural controls on fluvial distributary systems—The Luna System, northern Spain, *in* Ethridge, F.G., Flores, R.M., and Harvey, M.D., eds., Recent Developments in Fluvial Sedimentology: Society of Economic Paleontologists and Mineralogists Special Publication, p. 269–277.

Pareja, J., Vargas, C., Suárez, R., Ballón, R., Carrasco, R., and Villaroel, C., 1978, Mapa geológico de Bolivia y memoria explicativa: Yacimientos Petrolíferos Fiscales Bolivianos y Servicio Geológico de Bolivia, scale 1:1,000,000.

Pettijohn, F.J., Potter, P.E., and Siever, R., 1987, Sand and Sandstone (Second Edition): New York, Springer-Verlag, 553 p.

Reutter, K.J., Döbel, R., Bogdanic, T., and Kley, J., 1994, Geological map of the Central Andes between 20° and 26° S 1:1,000,000, *in* Reutter, K.J., Scheuber, E., and Wigger, P.J., eds., Tectonics of the Southern Central Andes: New York, Springer-Verlag, Enclosure 1.

Ridgway, K.D., and DeCelles, P.G., 1993, Stream-dominated alluvial fan and lacustrine depositional systems in Cenozoic strike-slip basins, Denali fault system, Yukon Territory, Canada: Sedimentology, v. 40, p. 645–666, doi: 10.1111/j.1365-3091.1993.tb01354.x.

Roeder, D., 1988, Andean-age structure of Eastern Cordillera (province of La Paz, Bolivia): Tectonics, v. 7, p. 23–39, doi: 10.1029/TC007i001p00023.

Sempere, T., 1995, Phanerozoic evolution of Bolivia and adjacent regions, *in* Tankard, A.J., Suárez, R., and Welsink, H.J., eds., Petroleum Basins of South America: American Association of Petroleum Geologists Memoir 62, p. 207–230.

Sempere, T., Hérail, G., Oller, J., and Bonhomme, M.G., 1990, Late Oligocene-early Miocene major tectonic crisis and related basins in Bolivia: Geology, v. 18, p. 946–949, doi: 10.1130/0091-7613(1990)018<0946:LOEMMT>2.3.CO;2.

SERGEOMIN (Servicio Nacional de Geología y Técnico de Minas), 1997, Mapas tematicos de recursos minerales de Bolivia, hoyas La Paz y Copacabana: Servicio Nacional de Geologia y Mineria, scale 1:250,000.

Smith, G.A., 2000, Recognition and significance of streamflow-dominated piedmont facies in extensional basins: Basin Research, v. 12, p. 399–411, doi: 10.1046/j.1365-2117.2000.00125.x.

Suárez, R., and Diaz, E., 1996, Léxico estratigráfico de Bolivia: Revista Técnica de Yacimientos Petrolíferos Fiscales Bolivianos, v. 17, p. 7–227.

Swanson, K.E., Noble, D.C., McKee, E.H., Sempere, T., Martinez, C., and Cirbian, M., 1987, Major revisions in the age of rock units and tectonic events in the northern Altiplano basin of Bolivia: Geological Society of America Abstracts with Programs, v. 19, p. 456.

Troëng, B., Soria, E., Claure, H., Mobarec, R., and Murillo, F., 1994, Descubrimiento de basamento Precámbrico en la Cordillera Occidental Altiplano de los Andes Bolivianos: XI Congreso Geológico de Bolivia, Santa Cruz, Memorias, p. 231–237.

Uba, C.E., Heubeck, C., and Hulka, C., 2005, Facies analysis and basin architecture of the Neogene Subandean synorogenic wedge, southern Bolivia: Sedimentary Geology, v. 180, p. 91–123, doi: 10.1016/j.sedgeo.2005.06.013.

Wörner, G., Hammerschmidt, K., Henjes-Kunst, F., Lezaun, J., and Wilke, H., 2000a, Geochronology (^{40}Ar/^{39}Ar, K-Ar and He-exposure ages) of Cenozoic magmatic rocks from northern Chile (18–22°S): Implications for magmatism and tectonic evolution of the central Andes: Revista Geológica de Chile, v. 27, p. 205–240.

Wörner, G., Lezaun, J., Beck, A., Heber, V., Lucassen, F., Zinngrebe, E., Rössling, R., and Wilke, H.G., 2000b, Precambrian and Early Paleozoic evolution of the Andean basement at Belen (northern Chile) and Cerro Uyarani (western Bolivia Altiplano): Journal of South American Earth Sciences, v. 13, p. 717–737, doi: 10.1016/S0895-9811(00)00056-0.

Manuscript Received 13 July 2009
Revised Manuscript Received 16 October 2009
Manuscript Accepted 23 October 2009

Printed in the USA